

A framework for capturing farm-scale variation in process-based simulations for agroecosystem resilience

Helen Metcalfe ^{*} , Kevin Coleman, Yusheng Zhang , Prakash N Dixit , Sana Saeed , Andrew Mead , Adrian L Collins

Rothamsted Research, West Common, Harpenden, Hertfordshire, AL5 2JQ, United Kingdom

ARTICLE INFO

Keywords:
Resilience
Spatial heterogeneity
Agroecosystem models
Farm-scale modelling
Modelling framework

ABSTRACT

Agroecosystem models typically simulate average conditions in fields or over a gridded landscape. This approach overlooks the spatial variation that shapes resilience at the farm scale. Yet, this variation can strongly influence production and regulating services, and their robustness to stresses. We developed a model-independent five-step framework for capturing farm-scale variation in process-based simulations for agroecosystem resilience. The framework comprises: 1) data acquisition; 2) data processing; 3) simulation; 4) output sampling, and 5) analysis and interpretation.

We applied the framework to two contrasting UK case exemplars, differing in climate, soils, and management. We used the Rothamsted Landscape Model to simulate calorific productivity, nitrate runoff and N₂O emissions. Simulations captured realistic farm-scale variability, including rare outcomes, reflecting the emergent effects of heterogeneous soils, weather, and farm management.

This flexible and transferable approach enables the simulation of agroecosystem performance and resilience using process-based models. It can help to explore system dynamics and risks at the farm scale under plausible spatial and temporal heterogeneity. By explicitly capturing these sources of heterogeneity at the scale most relevant for decision making, i.e., the farm, it provides a robust basis for applied research, policy design, and scenario exploration under current or future environmental change.

1. Introduction

Historically, agroecosystems research focused on developing strategies to improve net primary productivity, driven by the needs of a growing global population (Conway, 1987). Over time, the focus shifted toward sustainability, balancing productivity with environmental stewardship and resource conservation amid concerns over unintended consequences (Kleinman et al., 2018). Today, agricultural research, often takes a systems approach that integrates productivity with sustainability outcomes (Rao et al., 2004; Zhang et al., 2024). This includes frameworks that consider co-benefits and trade-offs between production, natural resource quality, profitability, and environmental impacts (Melchior and Newig, 2021).

Today, agriculture faces multifaceted challenges driven by socio-economic and environmental pressures. Unpredictable climate change and associated stresses, like pervasive soil degradation, threaten agroecosystems (Lal, 2021). Extreme weather events, like droughts and

heavy rainfall, are becoming more frequent and intense, damaging crops and the environment, and indirectly affecting food prices and availability (Calzadilla et al., 2013). Climate change is also shifting pest and disease distributions, increasing infestations and crop losses (Yang et al., 2024). Geopolitical tensions, including US–China trade disputes and the recent war in Ukraine, have disrupted global supply chains, making agricultural markets more vulnerable and prompting protective measures like grain export limits (Orehova and Ischuk, 2023).

Given this wide range of pressures on agroecosystems, it is increasingly important to explore and quantify resilience. Originally applied to ecological systems (Holling, 1973), the concept of resilience was later extended to socio-ecological systems (Folke et al., 2010; Walker et al., 2004) and agroecosystems (Darnhofer et al., 2010). Resilience is commonly defined as the ability to return to a stable state after disturbance (Davoudi et al., 2012; Scott, 2013) or more generally, to sustain (or improve) function over time (Pret et al., 2025). Variation within systems and among inputs and outputs in response to abiotic and biotic

* Corresponding author at: Rothamsted Research Harpenden, Hertfordshire United Kingdom.

E-mail address: helen.metcalfe@rothamsted.ac.uk (H. Metcalfe).

stresses is critical to understanding agroecosystem resilience comprehensively. Despite this, 47 % of farm-scale resilience studies cited in a 2025 review used only average-value metrics to assess farm performance (Pret et al., 2025). Critically, this can obscure variation such as very below-average performance during specific years (e.g., dry years).

To design innovative farming systems that support sustainable development and remain resilient to extant of predicted abiotic and biotic stresses, it is imperative to understand resilience drivers at the *farm scale* (Pret et al., 2025). This scale enables detailed insight into the manifold interactions and system dynamics shaping agroecosystem resilience, including how stresses, management, ecological functions, and socio-economic factors interact. It is also the main financial accounting and decision-making unit and is relevant to broader scale assessments (Hoy, 2015).

Field scale studies typically focus on productivity alone, as infrastructure for assessing other outcomes is often lacking, though exceptions do exist as exemplified by heavily instrumented strategic research platforms (e.g., Orr et al., 2016). Conversely, landscape-scale studies take a broader, often more environmental perspective given the routine strategic monitoring of environmental outcomes at such scales. Here, there can be a lack of attention to other farm performance metrics relevant to farmers, landowners, and policymakers. Even explicitly farm-scale studies often consider only one or two dimensions of farm performance (agronomic, economic, social, environmental), with few addressing three or all four (Pret et al., 2025).

Process-based models (PBM's) are frequently used to assess agroecosystem resilience. In a review of studies quantifying farm-based resilience, most relied on mechanistic crop, livestock, or farm models (55 %, $n = 42$; Pret et al., 2025). Models are valuable for simulating complex interactions and predicting system responses to environmental and management changes. They allow exploration of variation by generating multiple scenarios, unlike on-farm experimental studies. A wide range of PBMs now exist, ranging from process-specific models (e.g., RothC, Coleman and Jenkinson, 2014; DNDC, Giltrap et al., 2010), to systems-level models (e.g. APSIM, Holzworth et al., 2014; Daisy, Abrahamsen and Hansen, 2000), and fully integrated agroecosystem simulators (e.g., CSAmodel, Ren, 2019; Taghikhah et al., 2022). These models can each be used to explore different combinations of components of agroecosystem functioning. However, robust exploration of farm-scale resilience using any PBM(s), requires harmonized representation of farm-scale variability in model inputs and robust analysis of outputs. Recent discussions, across the wider modelling community, have highlighted persistent deficiencies in how modelling exercises are scoped and structured, particularly in defining model purpose, system boundaries, and scales of analysis. We therefore present a model-independent framework for capturing and analysing farm-scale variation in process-based agroecosystem simulations. (Jakeman et al., 2024). Our framework explicitly addresses two key challenges in modelling resilience: i) representing the diversity of real-world farm systems at the decision-making scale, and ii) analysing variability in outputs to assess resilience across multiple dimensions. This improves model transparency, reproducibility, and interpretability across diverse agricultural systems and model implementations. The framework is structured as a generic five-step workflow that is applicable across diverse agricultural systems, locations, and models. We demonstrate its application at two UK case exemplar sites using a single PBM, but the approach is designed for use with any compatible PBM or ensemble of models.

This framework enables users to: i) integrate and harmonize variation in soils, weather, crop rotations, and management into model inputs; ii) construct plausible virtual farmed landscapes from model outputs, and iii) assess full outcome distributions to identify both average performance and extreme responses critical to understanding and exploring agroecosystem resilience more comprehensively.

2. Methods

2.1. Generic framework

We developed a model-independent five-step framework (Fig. 1) to structure simulations of farm-scale variation using agroecosystem PBMs. It can be applied to both real farms with known characteristics and 'typical' farms at a given location, even where detailed site information is limited. We refer to the "site" as the location being simulated—either a specific farm or a virtual representative of the local farmed landscape. The framework captures variation often overlooked in traditional site-based parameterisation.

This framework formalises both the problem scoping and conceptualization phases of the modelling process (Jakeman et al., 2024). In line with good modelling practice, it integrates existing data, literature, and expert knowledge to identify key drivers of variation and determine appropriate system boundaries and scales of analysis. This ensures that conceptual assumptions are explicit, traceable, and transferable across different agroecosystem PBMs and study contexts.

These five steps operationalize best-practice good modelling principles across the modelling cycle: from explicit problem scoping and conceptualization through to transparent simulation and reproducible evaluation. Together, as a framework, they address several long-recognised gaps in agroecosystem modelling workflows (Grimm et al., 2014; Jakeman et al., 2006; Wang et al., 2023).

2.1.1. STEP 1: data acquisition

The data acquisition phase serves not only to gather inputs, but also to formalize the conceptual model of the system by defining which processes and drivers are most relevant to the problem being investigated. This reflects the "problem conceptualization" stage of good modelling practice (Jakeman et al., 2006), ensuring that choices about system boundaries, inputs, and scales are grounded in both system understanding and data availability.

Agroecosystem processes are shaped by spatial and temporal variation in land structure, farming system, weather, soils, and management. Input data to PBMs should reflect local heterogeneity in these factors, while retaining site specificity. Achieving this balance often requires collecting data from beyond the farm boundary. We recommend using the surrounding hydrological catchment as a pragmatic data acquisition zone as catchments provide a natural spatial unit that integrates both environmental processes and agricultural decision-making contexts. For many countries, the necessary datasets are available at catchment or regional scale (Table 1).

Farm and field areas: Acquire data on typical farm and field size distributions within the data acquisition zone. The size and structure of farms influences variation in outputs: small farms with few fields are more sensitive to outliers, whereas large farms tend to average out variability across fields.

Farming system: Describe land use classes and dominant production systems (e.g. livestock/arable). If unavailable at the site level, use catchment-scale census or land use data to infer local configurations.

Weather: Obtain meteorological data from a nearby weather station at the temporal resolution required by the PBMs, or at the highest temporal resolution available. Long time series help capture interannual variation.

Soil properties: Collect soil series data for the data acquisition zone (spatially explicit soil mapping units defined in national or regional soil surveys). Include all soil series that cumulate up to and including 65 % of total data acquisition zone area to capture key variation while limiting model complexity. For each soil series, extract required profile properties (e.g. texture, bulk density, organic matter content) for all soil horizons.

Agricultural management: Assemble data on typical crop types, livestock, and practices. If catchment-scale data are lacking, use national datasets or best practice guidelines to infer typical local farm

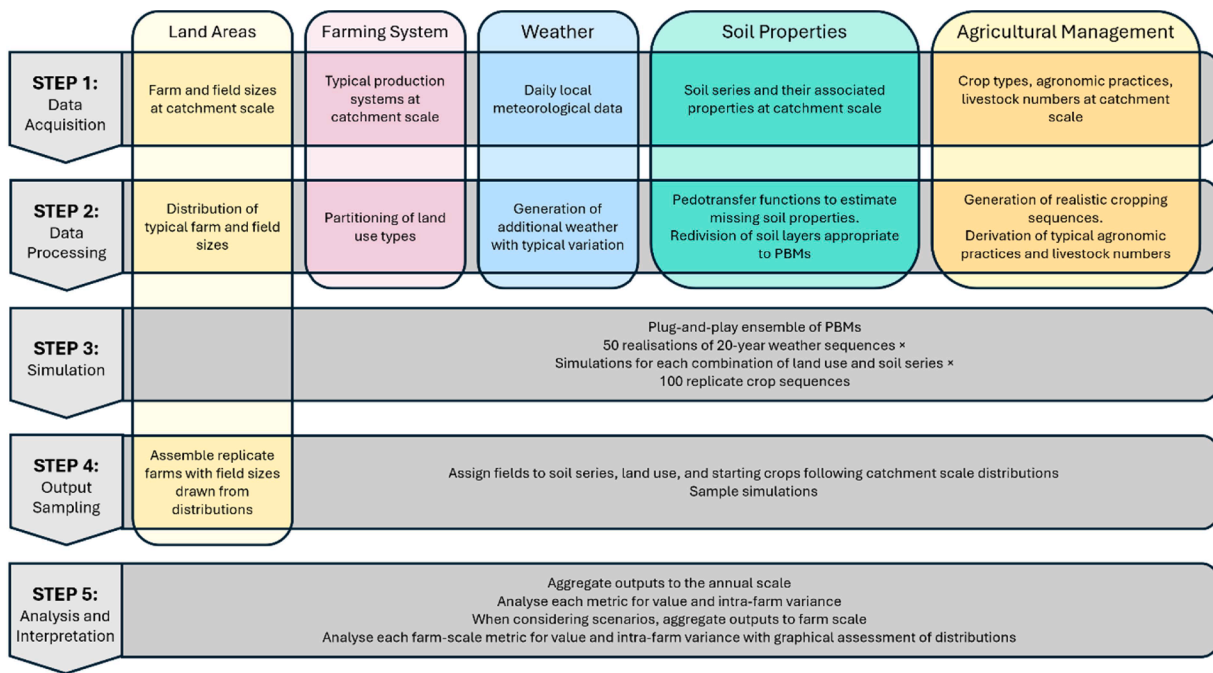


Fig. 1. A generic framework for capturing variation at the farm scale in process-based model simulations. The framework comprises 5 steps and utilises freely available or licensed data to describe land areas, farming systems, weather, soil properties, and agricultural management.

management.

2.1.2. STEP 2: data processing

Acquired data often require processing before use in PBMs.

Farm and field areas: To simulate realistic variation, fit frequency distributions to observed farm and field sizes. If data are limited, use median or mean values, though this omits variability. For richer datasets, simulate farms at key quantiles, (e.g. minimum, median, maximum). Field sizes can be categorised into nominal size classes (e.g. 1–2 ha, 2–3 ha, etc.) with mean or median values used to represent each class.

Farming systems: Where multiple systems exist at a site, simulate the dominant one or model each separately if resources allow. Partition land use based on the farming system type: arable farming systems typically allocate all land to cropping; upland grazing farms are mainly permanent grassland, and mixed farms have both (see Table 2). Where detailed information on farm composition is available, the framework can represent mixed or complementary systems directly by allocating land areas to both cropping and grazing enterprises. For undescribed or ‘typical’ farms where such data are unavailable, the dominant farming system is simulated to maintain site representativeness while avoiding unverified assumptions about enterprise complementarity. We acknowledge that this may be a limitation in regions where mixed systems are prevalent and detailed farm data are lacking.

Weather: Weather is a critical source of variation and a constraint on replication. Using weather data from additional locations or time periods can introduce bias. Tools like LARS-WG (Semenov and Barrow, 1997, 2002), CCWorldWeatherGen (Jentsch et al., 2013), and MarkSim (Jones and Thornton, 2013) generate synthetic weather representative of local conditions and can simulate future scenarios based on global circulation models (e.g., Semenov et al., 2024).

Soil properties: Soil profile data should be converted to model-ready inputs. Apply pedotransfer functions (e.g. Wösten et al. (1999)) to estimate unmeasured properties. Standardise varying layer depths to match PBM requirements using a weighted matrix. Let the observed profile have n layers with depth intervals defined by upper and lower bounds $[u_i, l_i]$, where $i = 1, 2, \dots, n$ and the model requires m layers with depth intervals $[U_j, L_j]$, where $j = 1, 2, \dots, m$. Compute an $m \times n$

matrix W such that each element $W_{j,i} \in [0, 1]$ represents the proportion of the j th model layer that is composed of the i th observed layer:

$$W_{j,i} = \frac{\min(L_j, l_i) - \max(U_j, u_i)}{L_j - U_j} \text{ if there is overlap, else } W_{j,i} = 0, \quad (1)$$

Let p_i be the value of a soil property in the i th observed layer. Compute P_j for the j th model layer as a weighted average:

$$P_j = \sum_{i=1}^n W_{j,i} p_i \quad (2)$$

Agricultural management: PBMs typically simulate pre-described crop sequences. These can be defined using catchment data, but real rotations are not typically static. Probabilistic crop sequence generators (e.g. Sharp et al. (2021)) use transition matrices and agronomic rules to replicate typical cropping patterns. These probabilistic crop sequences incorporate observed transition probabilities and agronomic rules (e.g., maximum number of consecutive same-crop sequences for disease management), thereby reflecting common patterns of complementarity among crops and pasture phases.

Additional agricultural management data (e.g. agrochemical inputs, in-field operations, stocking densities) should be translated into best-practice schedules aligned with PBM input requirements.

2.1.3. STEP 3: simulation

The simulation step operationalises the model formulation and implementation phases of good modelling practice (Jakeman et al., 2024). By defining simulations through transparent and modular input sets (generated in steps 1 and 2), the framework allows the structure, assumptions, and parameterisation of the modelling process to be fully documented and reproducible. Replication and systematic input variation help to quantify process uncertainty and sensitivity, providing a foundation for subsequent evaluation and comparison across PBMs or sites.

Simulations should be run across a structured set of replicates to capture variation in key uncertainties. We recommend at least 100 replicates per soil × weather × land use combination. In rotational cropping simulations, each replicate should begin with a randomly selected starting crop (based on data acquisition zone crop type

Table 1

Example data sources for key input categories relevant to simulating agro-ecosystem processes. Dataset, sources, and spatial coverage are provided for each of the five input categories described in step one of our framework.

Input category	Dataset	Coverage
Farm and field area	Land Cover + Crops (Land Cover plus: Crops, 2023)	Great Britain
	Agricultural Census (Government of India, 2025)	India
	USDA Census of Agriculture (USDA, 2022)	USA
	UK Agricultural Census (Defra, 2021b)	England & Wales
	FAOSTAT structural farm data (FAO, 2020)	Global
	Brazil Agricultural Census (IBGE, 2017)	Brazil
	Defra Farm Business Survey (Defra, 2025b)	England
	FAOSTAT livestock statistics (FAO, 2020)	Global
	Livestock Census (Government of India, 2025)	India
	Local meteorological stations (Met office, 2025)	UK
Farming system	Agri4Cast (European Commission, 2025)	Europe
	APHRODITE precipitation (Yatagai et al., 2012)	Asia
	Global Historical Climatology Network daily (Menne et al., 2012)	Global
	Daymet (Thornton et al., 2022)	North America
Weather	NATMAP Soil Series (LandIS, 2024)	England & Wales
	SoilGrids (Hengl et al., 2017)	Global
	Soil Atlas of Africa (Thiombiano et al., 2013)	Africa
	SOTERCAF (Van Engelen et al., 2006)	Central Africa
Agricultural Management	SSURGO (USDA, 2025)	USA
	ASRS (CSIRO, 2024)	Australia
	Land Cover + Crops (Land Cover plus: Crops, 2023)	Great Britain
	Farm Practices Survey (Defra, 2025c)	England
	FAOSTAT crop production data (FAO, 2020)	Global
	GloRice (Xie et al., 2025)	Global
	British Survey of Fertiliser Practice (Defra, 2023)	Great Britain
	FAOSTAT fertiliser/pesticide statistics (FAO, 2020)	Global
	AfricaFertilizer Database (AfricaFertilizer, 2015)	Sub-Saharan Africa
	FAOSTAT livestock numbers (FAO, 2020)	Global

Table 2

Typical proportion of land assigned to permanent grassland and rotational cropping for selected farming systems found in the UK.

Robust Farm Type ¹	Proportion of land assigned to permanent grass	Proportion of land assigned to rotational cropping (including grass leys)
Cereals	0	1
General Cropping	0	1
Lowland Grazing	0.75	0.25
Livestock		
Less Favoured Area	1	0
Grazing Livestock		

¹ Defra, 2010. Definitions of Terms Used in Farm Business Management, 3rd ed. Defra, London, pp. 48.

frequencies), followed by a uniquely generated crop sequence. To capture interannual variability and estimate medium-term resilience, simulations should run for at least 20 years.

The framework is designed to accommodate different PBMs, which inherently vary in structure and parameterisations. Even with identical inputs, they may produce divergent outputs due to differences in process

representations (e.g. crop growth, water balance, pest dynamics, nutrient cycling and loss). If multiple PBMs are available, simulations should be run in parallel using the same input datasets. While true ensemble modelling (statistical combination of outputs) is ideal, it may be unsuitable due to differing model structures and output formats. Nonetheless, applying a consistent simulation protocol across models enables comparison of model behaviours and output distributions. This reveals how structural assumptions influence predictions under common inputs. Incorporating variation in weather, soils, and management within and across models improves realism and supports more robust interpretable results.

2.1.4. STEP 4: model output sampling

Using land area data from steps 1 and 2, construct multiple simulated utilised areas (SUAs), each representing a virtual replicate farm, typical of the landscape. Total farm area, field number, and field sizes should be sampled from data acquisition zone distributions. If data are sparse, mean or representative values may be used. Independently assign each field within an SUA, a land-use type, soil series, and starting crop, sampled from the respective catchment-scale marginal distributions to reflect realistic heterogeneity (Fig. 2). Allocate pre-generated model outputs (from Step 3) to each virtual field, based on soil type and initial crop. Each replicate simulation should appear only once per SUA. Model outputs (per unit area) should be weighted by field area and aggregated to the farm scale for each SUA. We recommend creating a minimum of 10 SUAs per farm size class (e.g. small, medium, and large), depending on the study objectives and available data. The total number of SUAs is constrained by the number of unique simulations available per soil × crop type combination.

Variation among replicate simulations differs by land-use type. For cropped fields, each replicate includes a unique crop sequence. For permanent grassland, simulations may be near identical unless the PBM includes further stochastic elements. This should be considered when interpreting variability at the farm scale.

Due to the stochastic construction of SUAs, some rare combinations of soil, field size, and crop may not appear. This is intentional and supports generation of realistic outcome distributions.

Soil types were sampled proportionally to their relative area in the data acquisition zone rather than spatially interpolated and organised. This approach captures the dominant compositional variability in soil properties while avoiding assumptions about spatial connectivity, which are not represented in most agroecosystem PBMs. Because SUAs are used as aggregated, non-spatial farm units, proportional sampling provides a realistic basis for estimating farm-scale variation without introducing artefactual spatial structure.

We refer to these constructed entities as “simulated utilised areas” because many agroecosystem PBMs focus on crop and field processes, and do not simulate non-field infrastructure (e.g. farmyards, steadings, stores, tracks), despite the potential environmental impacts associated with the management of these elements of farm structure. The framework presented here captures variability in the productive land area, which typically accounts for most land use on farms and dominates ecosystem service delivery. This step supports transparent evaluation of model outputs by standardising their extraction and aggregation, enabling reproducible comparison across models, scenarios, or sites. By harmonising outputs within a consistent sampling framework, the approach mitigates one of the major barriers to inter-model comparison identified in previous studies (Jakeman et al., 2024).

2.1.5. STEP 5: analysis and interpretation

The analysis methods should match the study’s objectives. For comparisons (e.g., between sites, years, or scenarios), ANOVA can test differences in mean farm-scale responses. To ensure robust and representative results, input variability (e.g., weather, soil, field size aggregation) must be replicated. However, large simulation datasets can produce high statistical power, increasing the likelihood of detecting

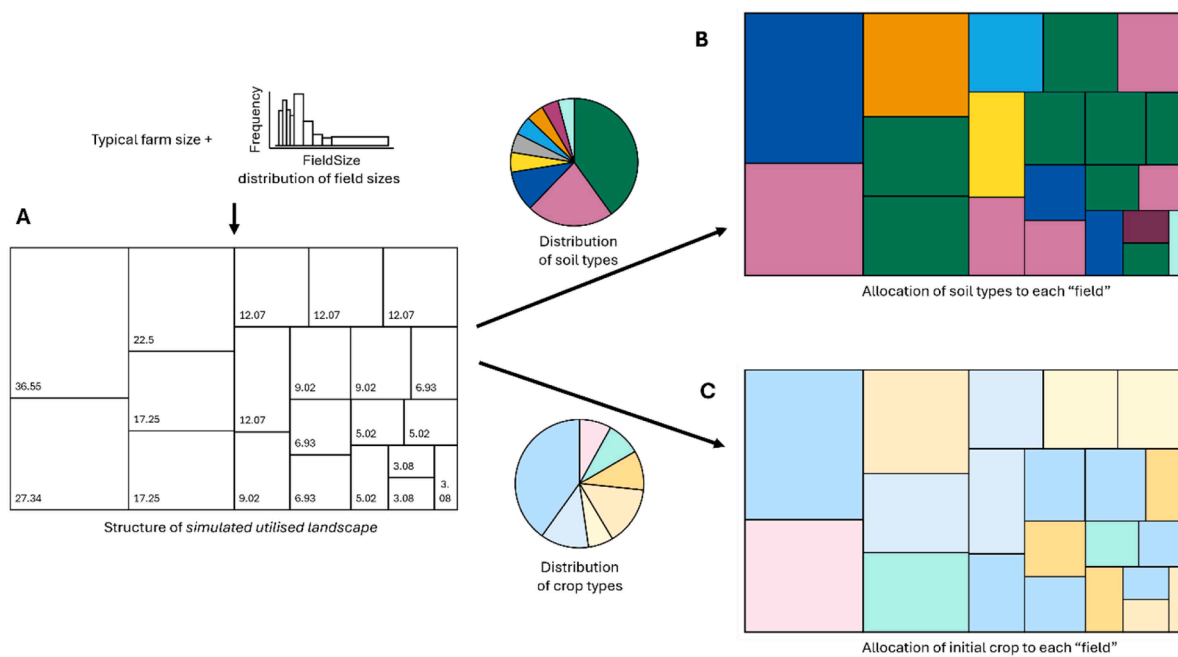


Fig. 2. Example composition of a “simulated utilised area”, representing a virtual medium-sized farm from the RR exemplar site. A) fields of varying sizes drawn from a categorised field size distribution of catchment-scale data. Each field is independently assigned B) a soil series, and C) an initial crop, sampled from the marginal distributions of soil series and crop types across the catchment. Not all combinations will be present in each replicate. For example, the grey soil in B does not appear in this SUA. Soil types were sampled proportionally by area from the data acquisition zone rather than spatially interpolated, as most PBMs simulate local processes independently of lateral field connectivity. This approach captures representative within-farm variation appropriate for aggregated SUA-level analyses. The configuration of fields within the figure does not indicate any spatial associations between fields.

statistically significant but practically trivial effects. Therefore, both statistical and practical significance should be considered.

For resilience assessments, variance and temporal dynamics are important. Alongside mean comparisons across years, it is informative to assess interannual variability using variances, standard deviations, or coefficients of variation (CV). These should be calculated per realisation (i.e. per SUA \times weather set) and compared using ANOVA or other appropriate tests, with the same caution about overpowered results. It is important to note that resilience in this context reflects stability of simulated outcomes, not persistence of higher yield and/or lower environmental burden.

To address the issue of overpowered tests, alternative approaches can explore the full distribution of outputs. One option is to fit parametric distributions to the generated data and analyse fitted parameters via ANOVA, assuming data fit standard distributions. Alternatively, non-parametric tests like the Kolmogorov-Smirnov test can compare pairs of empirical distributions, but extensions to more complex sets of distributions are not yet available. In such cases, graphical comparisons and

quantile summaries can aid interpretation, particularly when focusing on extremes that might be masked by means.

2.2. Application of the framework to two exemplar sites

To evaluate the robustness and applicability of our simulation framework, we applied it to two contrasting UK agroecosystems. These sites were selected to test the capacity to capture diverse sources of variation and to simulate plausible farm-scale outcomes under different environmental and farming contexts.

The exemplar sites (Fig. 3) are Harpenden (RR) in Hertfordshire ($51^{\circ} 48' N, 0^{\circ} 21' W$) and North Wyke (NW) near Okehampton in Devon ($50.77^{\circ} N, 3.92^{\circ} W$). These locations span an East-West climatic gradient and differ in rainfall, soil texture and farming systems. RR is an arable production area, whereas NW is pasture-based with lowland grazing livestock. Both sites are established experimental farms with comprehensive historical records, which we deliberately did not use in the simulation setup to test how well our generic approach can recreate

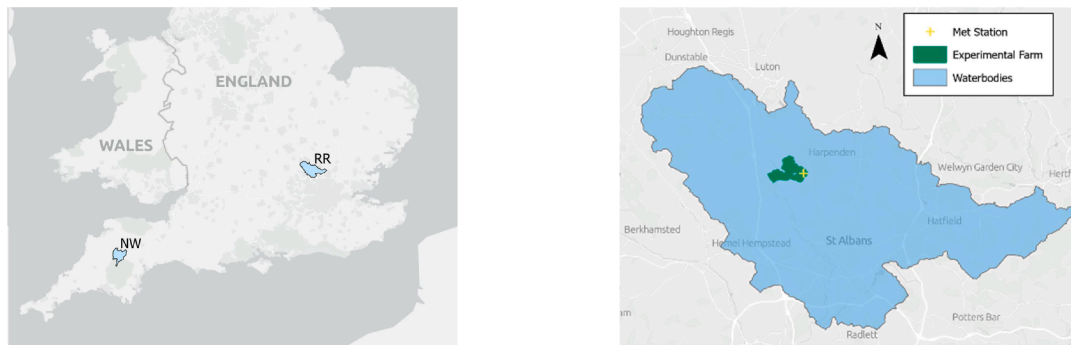


Fig. 3. The location of the waterbodies surrounding each of the two sites. B) Site RR shows an example of the Met station defining the site location within its surrounding waterbodies. The experimental farm is one example of a typical farm at this site.

local variation based solely on our data acquisition process.

2.2.1. STEP 1: data acquisition

We delineated the data collection zone at each site by identifying all European Union Water Framework Directive (WFD) waterbody catchments within a 5 km radius (Defra, 2025a); Fig. 3), excluding waterbodies with <10 % overlap. Each data-collection zone may therefore include multiple catchments. Finer hydrological units were not explicitly delineated because our framework is data-driven, and such data are rarely available at national scale. However, the WFD waterbodies used here integrate the effects of underlying micro-catchments, meaning that local hydrological variation is implicitly represented within the aggregated catchment-level inputs.

Typical farm size data were sourced from the UK agricultural census (Defra, 2021b), where average values are reported at the WFD waterbody scale. Field size distributions were derived from spatial land cover maps (Marston et al., 2022) by extracting all polygons designated as agricultural land within each data-collection zone.

Farming system data were also sourced from the UK agricultural census (Defra, 2021b), which reports the proportion of holdings associated with each Robust Farm Type (RFT) at the WFD waterbody scale. RFTs are defined based on dominant standard outputs, e.g., 'cereals' for wheat and barley producers, or 'mixed' for farms combining arable and livestock production.

Observed daily weather data were collected for 1985–2015 from site-based meteorological stations (Semenov et al., 2024), including minimum and maximum temperature (°C), precipitation (mm) and solar radiation (MJ m⁻²). Vapour pressure and wind speed were estimated using the methods of Allen et al. (1998).

Soil data were obtained from NATMAP 1000 (LandIS, 2024); a national 1 km resolution dataset of soil series across England and Wales. For each catchment we extracted the dominant soil series and corresponding soil properties relevant to either grassland (NW) or agricultural land (RR).

Crop types were characterised using Landcover PLUS crops maps (Land Cover plus: Crops, 2023) which provide estimates of annual crop classifications over five years (2018–2022). Fields classified as grassland across all five years were treated as permanent grassland and excluded. Additional management assumptions like sowing dates, fertiliser application rates, and other agronomic practices were derived from national guidelines, including the British Survey of Fertiliser Practice (Defra, 2019, 2020, 2021a, 2022, 2023). For NW, livestock numbers were based on the lowland grazing livestock RFT and included both temporary and permanent pasture (Defra, 2021b).

2.2.2. STEP 2: data processing

Farm size data were limited (typically only 3–4 values per WFD waterbody), so we used the mean, minimum and maximum values to define three representative farm sizes at each site. We constructed empirical field size frequency distributions by grouping fields into nominal categories (e.g. 1–2 ha, 2–3 ha, etc.) and calculated the mean field size within each. We used these to estimate the number of fields per farm. We then allocated fields to size categories in proportions that reproduced the empirical distribution as closely as possible.

At each site, the dominant RFT from the catchment was used to assign a representative farming system. At RR, this was 'cereals', and we assumed all land was under arable management. At NW, the dominant RFT was 'lowland grazing livestock' for which we assumed 75 % of the land was permanent grassland, and the remaining 25 % was cropped for livestock feed (Table 2).

Observed daily weather data were used to generate synthetic weather series using LARS-WG 8.07.0 (Semenov et al., 2024). For each site, we generated 1000 realised years of synthetic daily weather, then divided the output into 50 replicate sets of 20 years.

Soil series were selected to cumulatively represent at least ≥65 % of the catchment area. Soil profile properties were standardised into three

uniform depth layers (0–23 cm, 23–46 cm, 46–100 cm) as required by the PBM used in this study.

Crop sequences were generated using the generator developed by Sharp et al. (2021). We rescaled their transition matrices to represent only the crops observed in each catchment. This provided cropping sequences that reflect local agronomic conditions and practice more closely than regionally averaged transition probabilities.

2.2.3. STEP 3: simulation

To demonstrate application of the framework, we used the Rothamsted Landscape Model (RLM) to generate field-scale outputs for both exemplar sites. While these case studies employ a single PBM, for illustration, the framework is fully compatible with ensemble modelling, allowing multiple models with harmonised inputs to be run in parallel to assess structural uncertainty and improve robustness. In this study, we simulated a baseline "business-as-usual" (BAU) management scenario representative of current local practices (based on national and catchment-level datasets). The framework is, however, designed to support scenario testing including comparison of alternative management options (e.g., modified crop rotations, fertiliser strategies, tillage intensity, or grazing regimes). Such scenarios can be implemented by substituting or parameterising the relevant management input datasets. While scenario testing is beyond the scope of the present study, this capability will be applied in future work to evaluate the resilience implications of agri-environmental interventions.

2.2.3.1. Demonstration model: Rothamsted landscape model (RLM). RLM is a daily timestep PBM developed to simulate crop production and environmental impacts across field and farm landscapes (Coleman et al., 2017). It incorporates established modules including RothC (Coleman and Jenkinson, 2014), LINTUL (Wolf, 2012), and Century (Parton et al., 1994), supplemented by new routines, including an improved water model (Coleman et al., 2017). RLM has been calibrated and validated using long-term UK data.

RLM outputs a wide range of variables capturing both the productivity and environmental impact of the farmed landscape. For this study we focus on three contrasting indicators: calorific production (from crop and livestock outputs), nitrate losses via runoff, and N₂O emissions.

Each input dataset from Step 2 (soils, crop rotations, field layout, weather, and management) was formatted to meet RLM requirements. For each selected soil series at each site, we generated 100 replicate field-scale simulations. Each replicate combined a unique crop sequence (for arable land) with a randomly assigned starting crop and ran using one of 50 weather realisations (each spanning 20 years). Simulations began on 1st September and ran for 19 full cropping seasons. This created a structured simulation matrix capturing variation in soil, crop sequence, and weather. This matrix underpins the later construction of SUAs and supports analysis of both within- and between-site variation in farm-scale outcomes.

2.2.4. STEP 4: model output sampling

To explore variation at the farm scale, we generated 30 SUAs per site: 10 replicates each for small, medium, and large farm sizes based on farm size data from the data-collection zone.

For each farm size, we estimated the number of fields by dividing the farm area by the site-specific mean field size. Fields were then allocated to size categories to reflect the empirical distribution of field sizes at each site. Soil types and initial crops were then independently sampled for each field from the catchment-level discrete distributions (see Fig. 2, for the characteristics of an example SUA for a medium-sized farm at RR). This random allocation mirrors the heterogeneity in real farms and enables sampling across plausible combinations of land use and soils. Because field sizes, soil series, and initial crops are sampled independently, some rare combinations may not appear in every SUA, especially on smaller farms—this is intentional and reflects real-world variation.

Each field was assigned a model simulation from the corresponding pool of RLM outputs (Step 3), consistent with its soil type and initial crop. Simulation replicates were randomly permuted to ensure that no replicate was reused within a single SUA, though replicates could appear across multiple SUAs.

2.2.5. STEP 5: analysis and interpretation

Here, we use our case study sites to illustrate how modelled indicators can be aggregated and statistically compared using our framework. The analyses serve as examples of the types of evaluation possible and demonstrate how PBM outputs can be explored using a consistent, statistically robust approach. They are not intended to represent all relevant scientific questions.

To compare productivity across crop sequences and between arable and livestock systems, we converted crop yields and livestock outputs to calorific equivalents, accounting for losses from harvest to consumption (for methods see [Sharp et al., 2024](#)).

Nitrate runoff and N₂O emissions are outputted from RLM on a daily timestep. We calculated their sum over each cropping year. These were then used as response variables. Farm-level weighted means were calculated per SUA, and cropping year, using field area as the weights (from Step 4).

2.2.5.1. Assessing system performance. Each site produced 28,500 weighted mean responses (10 SUAs \times 3 farm sizes \times 50 weather sets \times 19 cropping years). We used ANOVA to assess variation in mean responses, testing null hypotheses that farm size, cropping year, and their interaction had no effect on calorific production, nitrate runoff and N₂O emissions. A hierarchical blocking structure was assumed: cropping years nested within weather sets, nested within SUAs. Farm size was assessed relative to the between-SUA variation and cropping year and the interaction were assessed relative to the between-cropping year variation.

2.2.5.2. Assessing system resilience. We quantified resilience as the temporal stability of SUA responses across years. For each SUA \times weather set \times response variable, we calculated the standard deviation (used in preference to variance to satisfy the ANOVA homogeneity of variance assumption), and a scale-adjusted coefficient of variation (aCV) following [Döring and Reckling \(2018\)](#), which removes dependence of the standard CV from the mean.

We combined datasets across sites to compare resilience at NW and RR. As farm size and weather sets were site-specific, a nested treatment structure was appropriate: weather sets nested within each of the 60 SUAs. Site, and farm size (within site) effects, were estimated at the between-SUA level; weather effects and their interaction with site at the between-weather set level. This enabled identification of specific weather realisations associated with poor resilience, potentially reflecting extreme weather events.

2.2.5.3. Distributions of outputs. With 500 SUA replicates per farm size per site, ANOVA was statistically overpowered. Nearly all effects appeared significant, even where practical or biological differences were negligible. To aid interpretation, we therefore used violin and box-and-whisker plots to visualise response distributions across cropping years and farm sizes.

2.2.5.4. Assessing sources of variation. In addition to the analysis recommended within step 5 of our framework, we additionally wanted to demonstrate, using our case study sites, the degree to which the collected input data represents both the absolute values and levels of variation observed on farms. We assessed both the realism of generated model inputs and the importance of different sources of variation.

Weather: We compared generated and observed weather data at each site using *t*-tests to compare monthly means (temperature,

radiation) and total (precipitation) values, and *F*-tests to compare monthly variances. We applied Kolmogorov-Smirnov tests to compare distributions.

Soils: Generated soil inputs were compared with published farm surveys, assessing soil series and associated properties.

Crop sequences: Annual area-weighted crop proportions were calculated for the experimental farm, the catchment, and SUAs. We plotted these as stacked bar charts for visual comparison.

Sources of output variation: We used ANOVA on field-level outputs (summarised annually, pre-SUA aggregation) to evaluate effects of soil type, weather set, and cropping years, including interactions. A hierarchical blocking structure was assumed: cropping years nested within weather sets, nested within soil types, nested within the 100 replicate runs comprising different cropping sequences. As with other analyses, *p*-values were interpreted cautiously due to high statistical power.

While the present implementation focuses on RLM outputs, the framework and analytical workflow are model-agnostic and can be applied across other agroecosystem PBMs given equivalent input and output structures.

2.2.5.5. Statistical packages. Daily RLM outputs were processed in R (v4.4.1; ([R Core Team, 2025](#)) using the data.table ([Barrett et al., 2025](#)), dplyr ([Wickham et al., 2025](#)) and future.apply ([Bengtsson, 2021](#)) packages. SUA construction, resampling, and ANOVA were conducted using Genstat (23rd Edition) ([VSN International, 2023](#)). Farm-level output summaries were computed in R. Scale-adjusted CVs were calculated using the metan R package ([Olivoto and Lúcio, 2020](#)). Graphics were generated in Genstat, and in R using the ggplot2 package ([Wickham, 2016](#)).

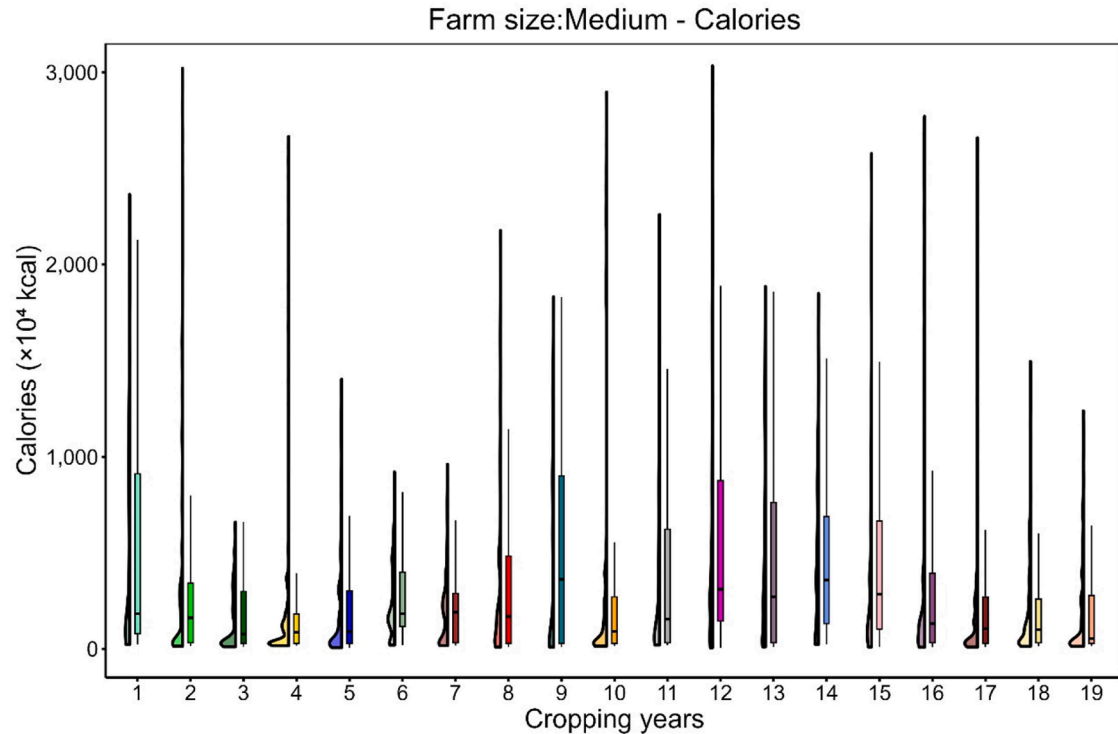
3. Results

3.1. Assessing system performance

Simulated calorific production varied widely between the two sites ([Fig. 4](#)) with RR producing more food than NW. Farm-scale simulated wheat yields at RR were comparable to farm measurements, whereas at NW simulated yields were approximately 3 t/ha higher. At both sites, simulated yields within SUAs were less variable than the observed data (see supplementary figure S1). NW showed greater variability in calorific production, with a few high-performing SUAs and many low performing ones ([Fig. 4B](#)). ANOVA identified no significant differences in calorific production across virtual farm sizes (RR: $F_{2, 27}=0.306, p = 0.739$; NW: $F_{2, 27}=0.148, p = 0.864$; supplementary figure S2). In contrast, both the cropping year main effect and the interaction effect between cropping year and farm size were significant (RR: cropping year $F_{18, 26,946}=218.042, p < 0.001$; interaction $F_{36, 26,946}=14.083, p < 0.001$; NW: cropping year $F_{18, 26,946}=41.727, p < 0.001$; interaction $F_{36, 26,946}=16.678, p < 0.001$). These effects likely reflect differences in generated cropping sequences and crop distributions across years (see [Fig. 9](#)), rather than weather variation, as all 30 SUAs per site shared 50 common weather datasets. The significant interactions almost certainly reflect the overpowered nature of the tests as the means across all three farm sizes were similar and so changes in their relative order are of little practical consequence (supplementary figure S2). Total simulated food production varied by year, and within-year variation among SUAs was also substantial ([Fig. 4](#)). At RR, distribution plots reveal distinct peaks, indicating strong effects of SUA composition on calorific output ([Fig. 4B](#)).

Simulated nitrate loss via runoff was typically lower at NW than RR ([Fig. 5](#)), with clear temporal fluctuations and a significant effect of cropping year (RR: $F_{18, 26,946}=208.329, p < 0.001$; NW: $F_{18, 26,946}=1438.474, p < 0.001$; supplementary figure S3). Variation among SUAs within years was substantial ([Fig. 5](#)). There was no significant farm size effect (RR: $F_{2, 27}=2.584, p = 0.094$; NW: $F_{2, 27}=0.023, p = 0.977$),

A



B

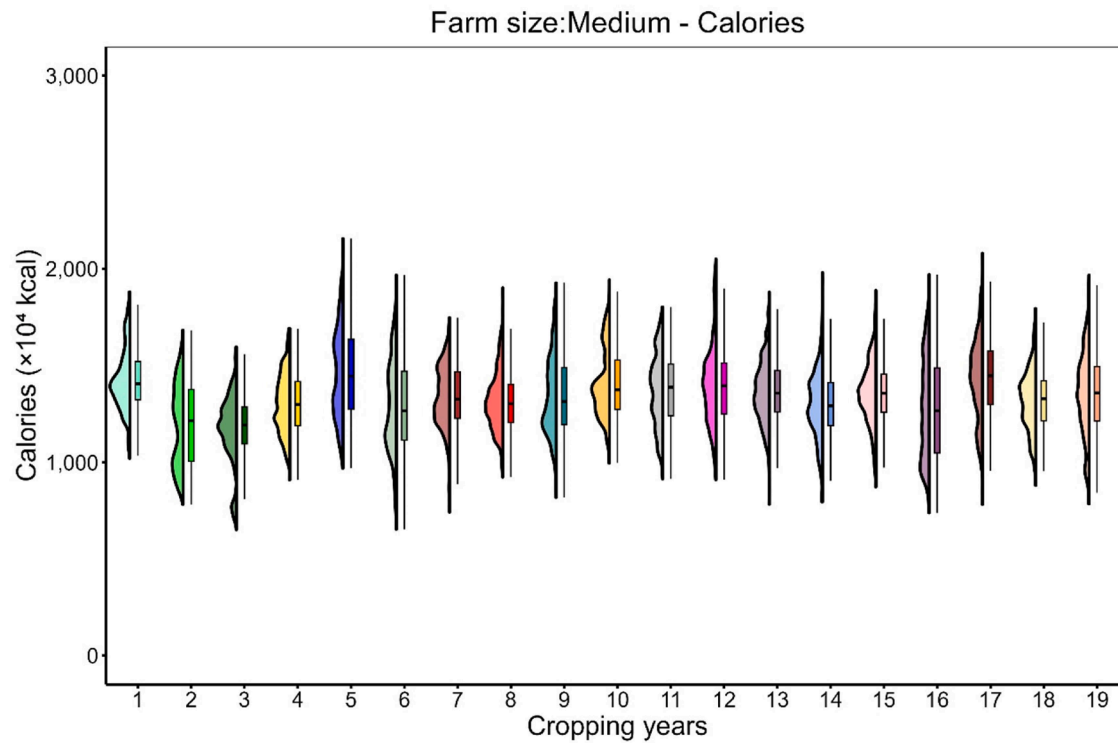
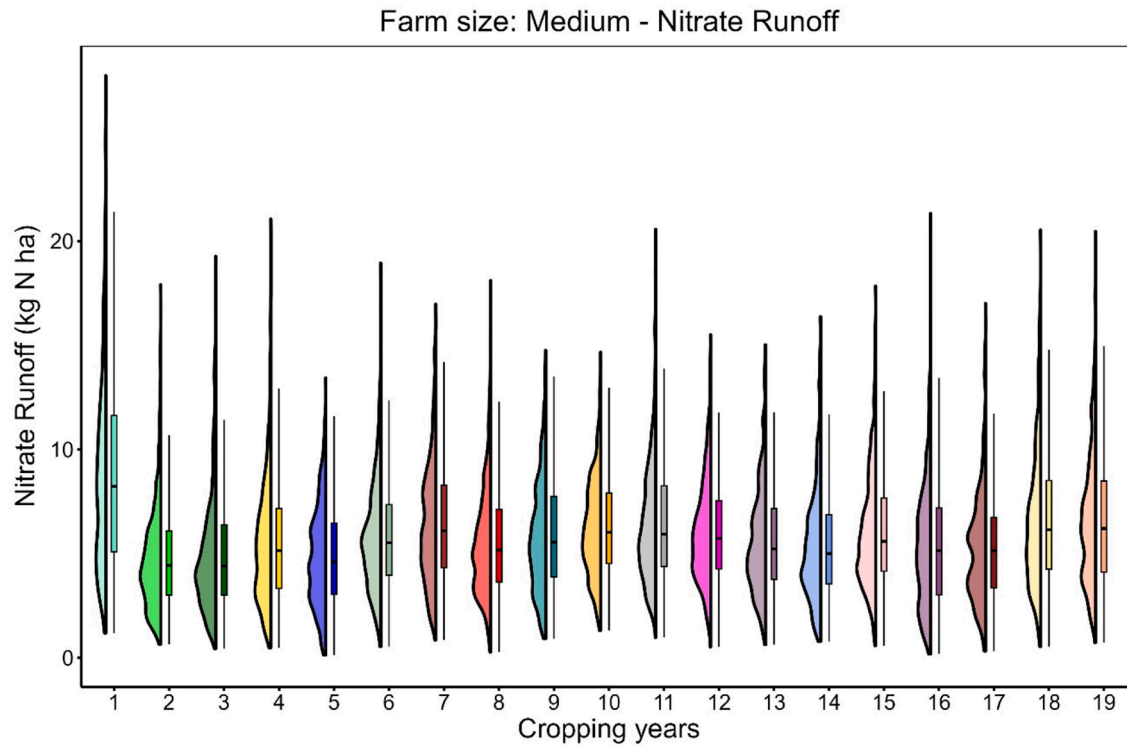


Fig. 4. Simulated calorific production across a sequence of 19 cropping years at A) NW and B) RR sites. Box and whisker plots show the median (black bar), interquartile range (IQR; box) and the smallest/largest values no further than 1.5 IQR from the first/third quartile (whiskers). Density plots indicate the distribution of SUA values. Values represent weighted means of combinations of individual field simulations constructed to capture the potential variation present between farms, and for 50 independently generated weather datasets.

A



B

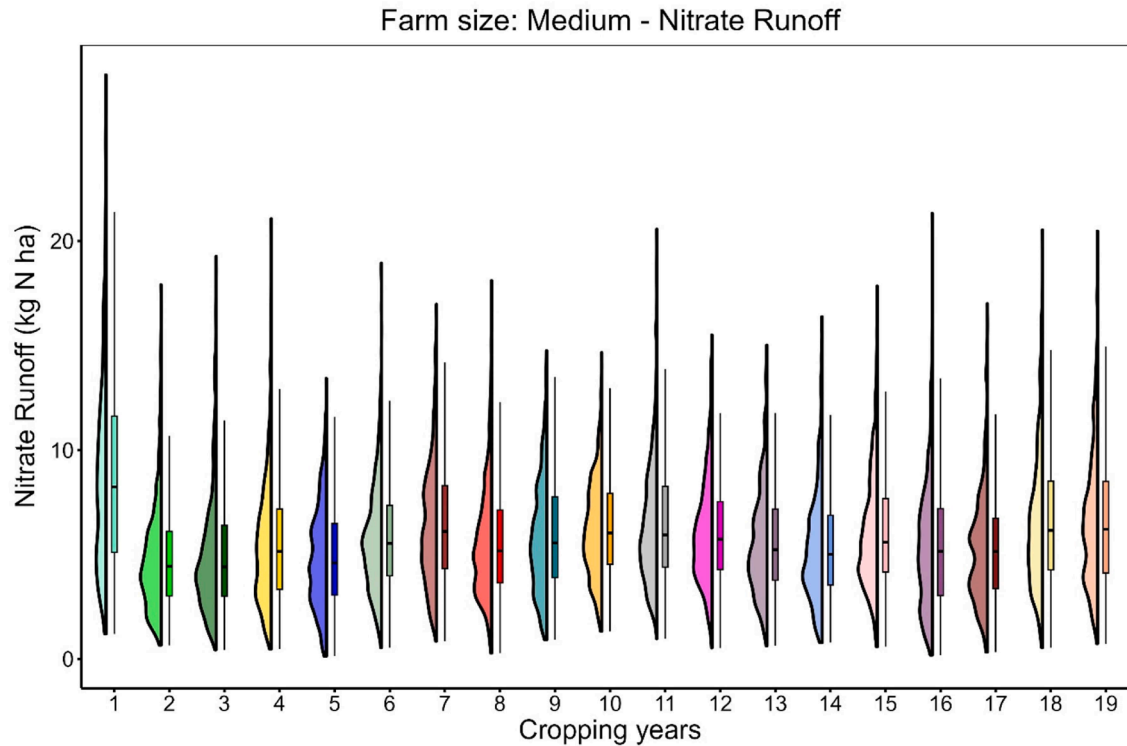


Fig. 5. Simulated nitrate runoff across a sequence of 19 cropping years at A) NW and B) RR sites. Box and whisker plots show the median (black bar), interquartile range (IQR; box) and the smallest/largest values no further than 1.5 IQR from the first/third quartile (whiskers). Density plots indicate the distribution of SUA values. Values represent weighted means of combinations of individual field simulations constructed to capture the potential variation present between farms, and for 50 independently generated weather datasets.

but small statistically significant interaction effects between cropping year and farm size (RR: $F_{36, 26,946}=5.791, p < 0.001$; NW: $F_{36, 26,946}=29.576, p < 0.001$).

N_2O emissions simulated using the framework also varied significantly by cropping year (RR: $F_{18, 26,946}=539.15, p < 0.001$; NW: $F_{18, 26,946}=522.557, p < 0.001$; supplementary figure S4), with no significant farm size effect (RR: $F_{2, 27}=1.341, p = 0.279$; NW: $F_{2, 27}=0.566, p = 0.575$) and small, but significant, interaction effects between cropping year and farm size (RR: $F_{36, 26,946}=18.878, p < 0.001$; NW: $F_{36, 26,946}=33.816, p < 0.001$). Emissions were generally higher at RR, with substantial within-year variation among SUAs, particularly at RR (Fig. 6).

These results illustrate how the framework can capture and compare farm-scale variability in modelled production and environmental outputs across contrasting sites, using harmonised inputs.

3.2. Assessing system resilience

Applying the frameworks resilience metrics to simulated calorific outputs revealed significantly more resilience in calorific production at RR than at NW, with lower SD and aCV values (SD: $F_{1, 54}=16.673, p < 0.001$; aCV: $F_{1, 54}=139.616, p < 0.001$; Fig. 7). No significant differences in farm-scale calorific production resilience were observed across farm sizes nested within site (SD: $F_{4, 54}=0.480, p = 0.750$; aCV: $F_{4, 54}=0.154, p = 0.960$), though this may reflect large variation among SUAs within each size category, especially at NW where the proportion of the total field area allocated to arable crops varied substantially between SUAs. Weather set (nested within site) had a significant, but modest, effect on calorific production resilience (SD: $F_{98, 2646}=3.042, p < 0.001$; aCV: $F_{98, 2646}=2.129, p < 0.001$). There was a small, but significant, interaction between farm size and weather sets for SD ($F_{196, 2646}=1.226, p = 0.021$), but no statistically significant interaction effect for aCV ($F_{196, 2646}=1.085, p = 0.207$).

These results suggest that calorific production resilience varies with weather patterns and that farm size can mediate this effect. At RR, large virtual farms were generally the most resilient, though under certain weather sets (e.g. 23, 44, 50), medium farms were more resilient (Fig. 7). At NW, where mixed systems were simulated, small virtual farms were the least resilient indicating that farm composition may be influential, with greater year-to-year variation in calorific production due to crop composition.

For simulated farm-scale nitrate runoff resilience, site had no significant effect on SD ($F_{1, 54}=0.271, p = 0.605$), but did affect aCV ($F_{1, 54}=31.692, p < 0.001$), reflecting similar SD at both sites, but higher mean nitrate runoff at RR than NW (Supplementary figure S5), reflecting the different crop compositions. Farm size (nested within site) did not have a significant effect for either metric (SD: $F_{4, 54}=1.078, p = 0.376$; aCV: $F_{4, 54}=0.832, p = 0.511$). Weather set (nested within site) significantly affected both nitrate runoff SD and aCV (SD: $F_{98, 2646}=94.259, p < 0.001$; aCV: $F_{98, 2646}=97.864, p < 0.001$), but there was no evidence of a site \times weather set interaction (SD: $F_{196, 2646}=1.072, p = 0.241$; aCV: $F_{196, 2646}=0.907, p = 0.812$).

The framework simulated farm-scale stability of N_2O emissions differed significantly between sites for SD ($F_{1, 54}=34.166, p < 0.001$) but not for aCV ($F_{1, 54}=0.702, p = 0.406$), with higher variability and emissions at RR (Supplementary Figure S6). There was no evidence for a farm size effect (SD: $F_{4, 54}=2.498, p = 0.053$; aCV: $F_{4, 54}=1.066, p = 0.383$). Weather set significantly affected both metrics (SD: $F_{98, 2646}=14.723, p < 0.001$; aCV: $F_{98, 2646}=96.391, p < 0.001$), but interaction effects between weather set and farm size were not significant (SD: $F_{196, 2646}=1.124, p = 0.122$; aCV: $F_{196, 2646}=1.085, p = 0.207$), indicating sensitivity to specific weather scenarios across farm sizes.

This demonstrates how the framework can be used to identify site- and weather driven differences in system stability, independent of PBM structure.

3.3. Assessing sources of variation

The framework input harmonisation allows weather, soil, and cropping variation to be explored systematically across sites.

3.3.1. Weather

Both sites followed typical UK seasonal temperature patterns. Daily maximum temperatures peaked in July–August, with no significant differences in monthly means between observed and framework-generated data (via LARS-WG) at either site (Fig. 8A). Minimum temperatures peaked in May–July (Fig. 8B), again with no significant differences in means between framework-generated and observed data. RR showed greater annual temperature variation, reflecting milder NW winters. Solar radiation peaked in July, more sharply at RR (Fig. 8C). January radiation was overestimated in the generated data (NW: $p = 0.010$; RR: $p = 0.003$). NW had higher, more winter-skewed rainfall, while RR's rainfall was more evenly spread (Fig. 8D). No significant differences between observed and generated monthly precipitation were detected, though variances were generally lower for generated data, significantly so in 4 months at NW and 3 months at RR. Kolmogorov-Smirnov tests suggested the monthly distributions of generated and observed weather were statistically similar.

Analysis of pre-aggregation model outputs (summarised for cropping years, but pre-SUA construction) confirmed that the framework successfully captures the sensitivity of outputs to underlying input variation. Weather set significantly affected calorific production, nitrate loss via runoff, and N_2O emissions, supporting the use of multiple weather realisations.

3.3.2. Soil characteristics

At NW, the experimental farm is dominated by Halstow series (Pelostagnogley soils, Avery, 1980; classified as Stagni-vertic cambisol under the FAO system and Typic haplaquept in US soil taxonomy). In contrast, Hallsworth series dominated our framework-generated SUAs, while Halstow covered only 8.9 % of simulated land (6.0 % of the catchment, Table 3). The two series are similar in clay content (Halstow: 34.0 %, Hallsworth: 39.5 %) but differ in silt (36.0 % vs 43.6 %), acidity (pH 5.8 vs. 6.8), and organic content (3.6 % vs. 3.2 %).

At RR, soils range from clay loam to silty clay loam; mainly Batcombe series (Avery and Catt, 1995; Avery et al., 2024; classified as Chromic Luvisol (or Alisol) by the FAO and Aquic (or Typic) Paleudalf in US soil taxonomy). Typical Batcombe covers 46.61 % of the RR farm, with Heavy Batcombe adding 6.71 %. In our framework-generated SUAs, Batcombe accounted for 40.1 % of land (26.2 % of the catchment, Table 3).

ANOVAs on pre-SUA model outputs revealed significant effects of soil series on all three modelled outputs, highlighting the importance of simulating multiple soil types at farm scale, and therefore the value of the framework in capturing the full potential variation in soils at the farm scale.

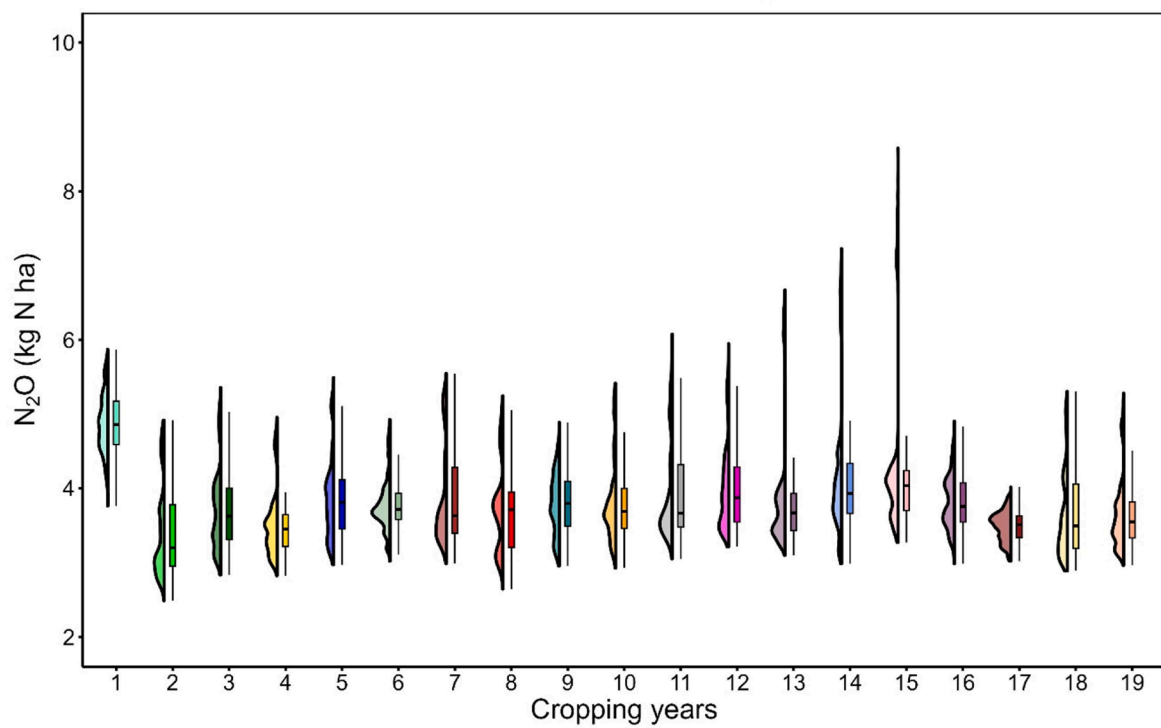
3.3.3. Cropping patterns

At NW, our framework identified the most likely farming system to be present as “lowland grazing livestock” and we therefore assumed 75 % of land was permanent pasture, with 25 % under arable rotation. Since 2019, about one-third of the experimental farm has been arable, growing winter wheat, winter barley, oats, and field beans (Fig. 9). These, crops along with grass leys and other crops (Table 3), were included in our simulations. The remaining land is used for pasture. The partitioning of land use derived using our framework corresponds well with the real land-use on the experimental farm at NW.

At RR, winter wheat dominates the catchment (33.5 %) and the experimental farm, though 2021 featured more spring wheat. Spring and winter barley are common in the catchment (12.4 % and 10.2 %), while oats were prominent on the experimental farm (Fig. 9).

Fig. 9 shows that catchment-level cropping is stable over time due to

A

Farm size: Medium - N_2O 

B

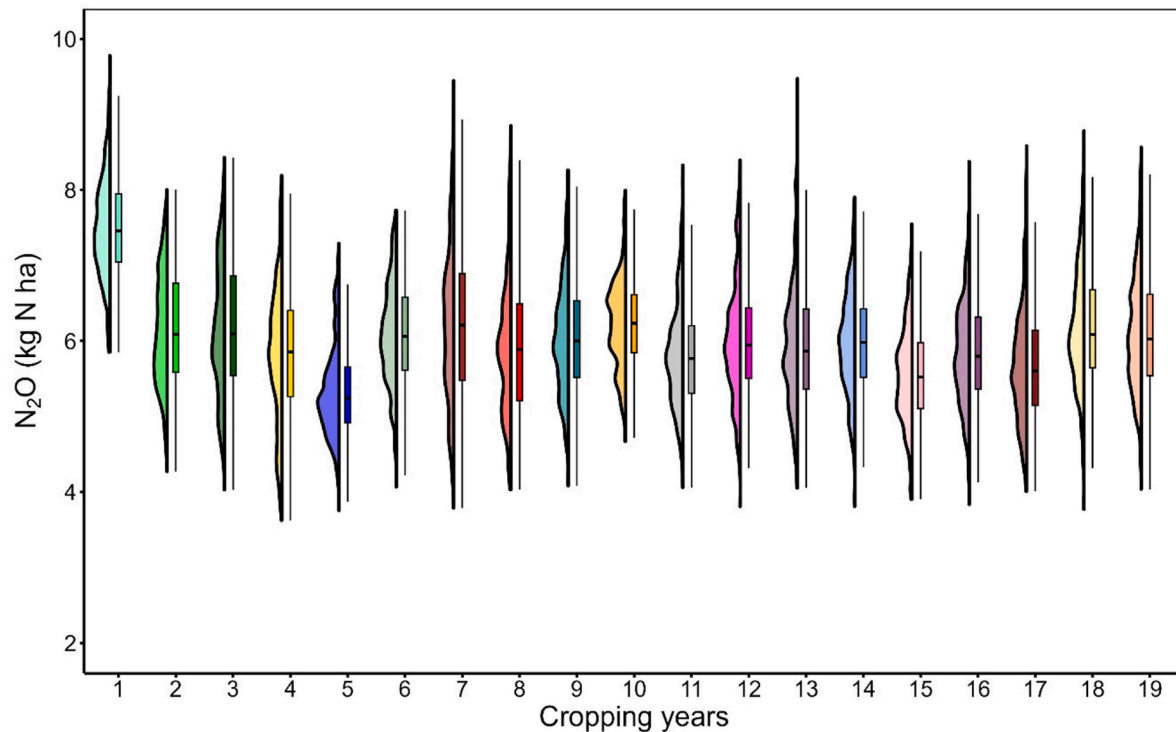
Farm size: Medium - N_2O 

Fig. 6. Simulated N_2O emissions across a sequence of 19 cropping years at A) NW and B) RR sites. Box and whisker plots show the median (black bar), interquartile range (IQR; box) and the smallest/largest values no further than 1.5 IQR from the first/third quartile (whiskers). Density plots indicate the distribution of SUA values. Values represent weighted means of combinations of individual field simulations constructed to capture the potential variation present between farms, and for 50 independently generated weather datasets.

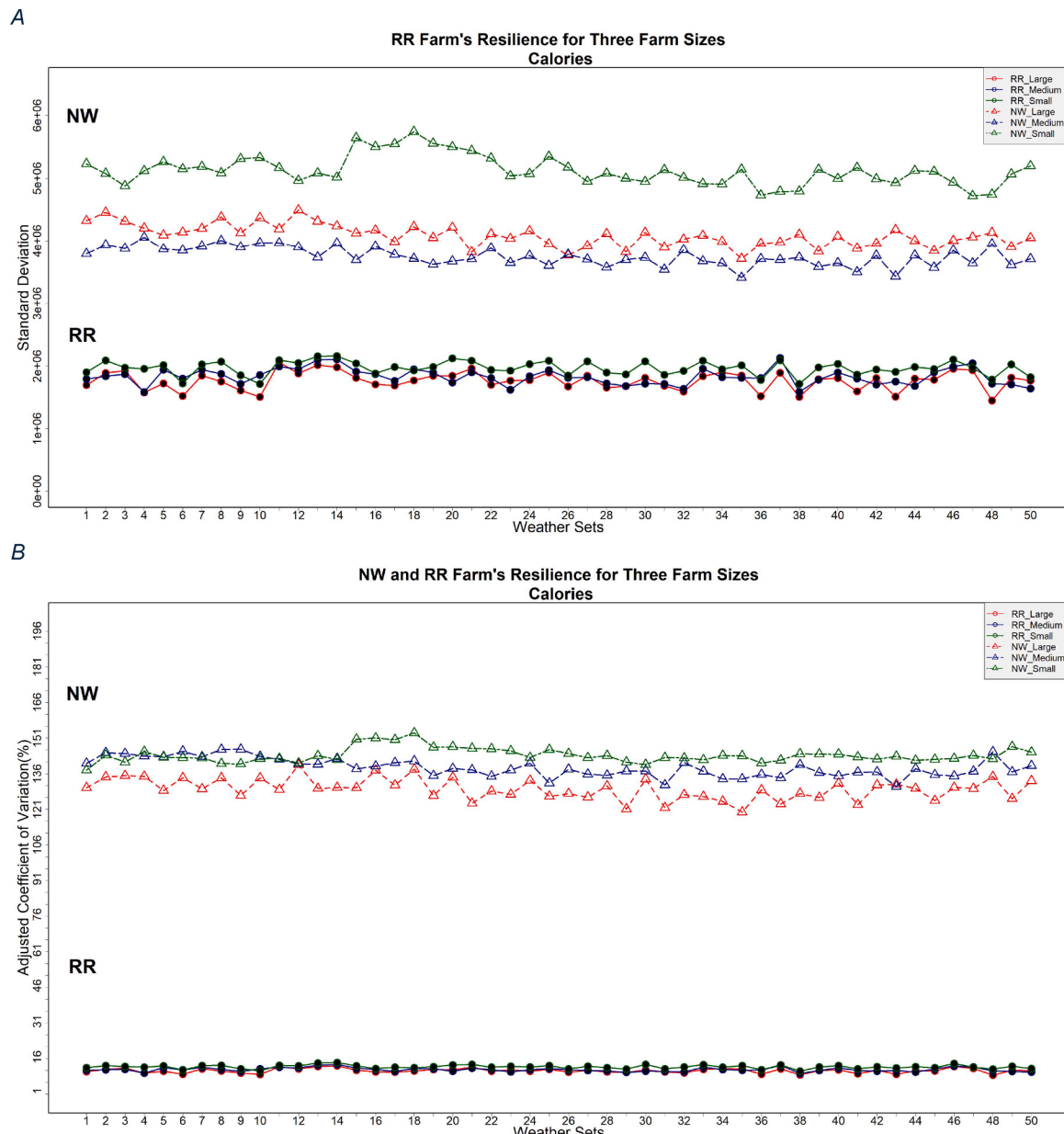


Fig. 7. Mean A) standard deviation (SD) and B) scale-adjusted Coefficient of Variation (aCV) of simulated calorific production across large (red), medium (blue) and small (green) farms at NW and RR sites. Each value is the mean SD/aCV across 10 SUAs for a site \times farm size \times weather set combination. Note that the actual sizes of large, medium, and small farms differ according to site. (For interpretation of the references to color in this figure legend, the reader is referred to the web version of this article.).

the larger spatial extent than the experimental farm. Our SUA approach reintroduces variability, better capturing farm-level variation than catchment data alone.

Across all analyses, the framework enabled consistent comparison of outcomes across data sources, revealing how farm-scale heterogeneity influences both mean performance and resilience metrics.

4. Discussion

We developed and applied a model-independent framework to simulate realistic within-farm variation in agroecosystem processes, designed to complement existing PBMs. By systematically integrating variation in soils, weather, crop sequences, and farm management into model inputs, we constructed plausible virtual farms (SUAs) and assessed full distributions of farm-scale outcomes, including extremes, to support resilience assessments. Input variation, typically absent from

modelling studies, strongly influenced model outcomes. Explicitly modelling this variation revealed how within-farm heterogeneity supports performance and resilience, aligning with previous findings on diversity and agricultural stability (Beillouin et al., 2019; Lin, 2011). In doing so, the framework advances current modelling practice by bridging existing PBMs and resilience assessment approaches, offering a transparent, reproducible, and transferable structure for exploring system behaviour under realistic variation.

The two exemplar sites (NW and RR) were selected to represent contrasting ends of a dominant UK agroecosystem gradient: pasture-based lowland grazing versus arable cereal production. This contrast tests the framework's capacity to capture and interpret diverse sources of variation across systems that differ in soils, climate, and management intensity. The shared set of resilience indicators provides a consistent basis for cross-system comparison, enabling lessons on how input heterogeneity and farm structure influence performance to be generalised

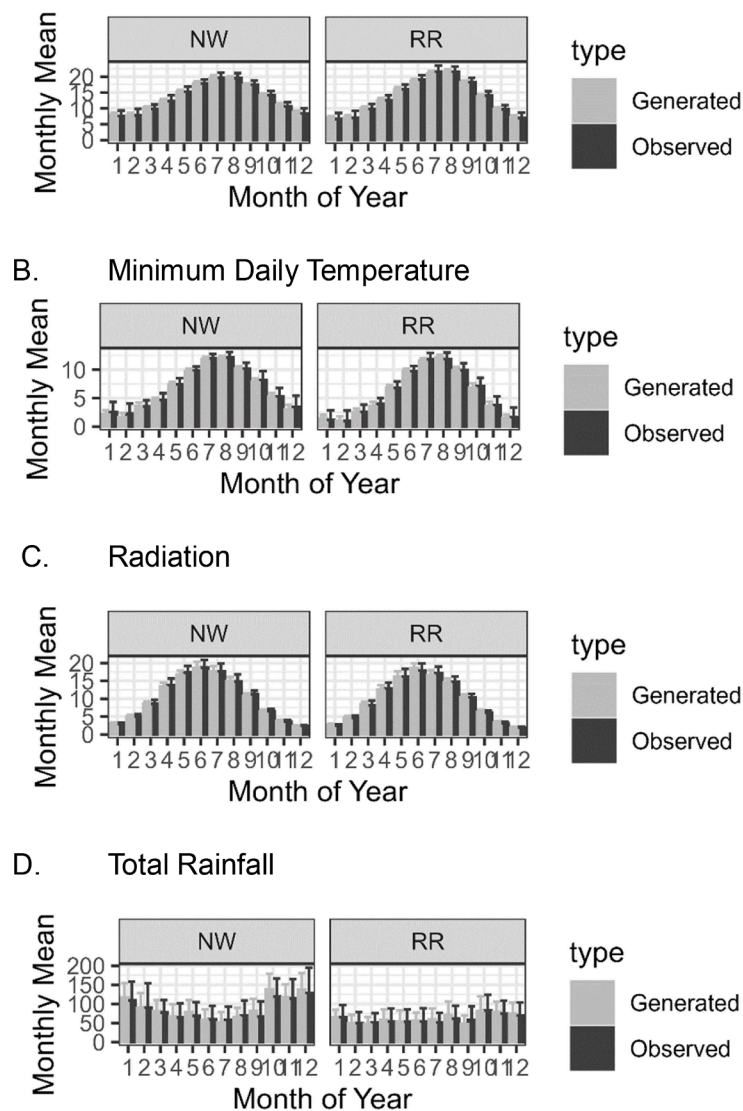


Fig. 8. Monthly mean weather variables at North Wyke (NW) and the Harpenden (RR) sites. Grey bars represent generated weather data, and black bars show observed measurements. Error bars indicate \pm standard error of the mean (SEM). (A) Maximum daily temperature, (B) Minimum daily temperature, (C) Solar radiation, (D) Total rainfall.

to other farms. Thus, while the absolute results are site-specific, the methodological insights are transferable, illustrating how the framework can be used to identify both common resilience mechanisms and context-dependent vulnerabilities.

Our results support the idea that diversity in soils, crops, and management creates functional redundancy, where poor performance in one component can be offset by others (Elmqvist et al., 2003). This heterogeneity enables persistence pathways that uniform systems lack, making them more vulnerable to shocks or variable stresses. Although high output variability may signal instability (Scheffer et al., 2009), input heterogeneity can instead reflect adaptive capacity when it buffers risk (Kotschy et al., 2015). Variation across SUAs buffered farm-level outcomes despite local failures, aligning with resilience concepts that emphasise both resistance and response capacity (Biggs et al., 2015). Capturing this complexity is essential; simpler models risk underestimating both vulnerabilities and adaptive potential.

Assessing full output distributions enabled nuanced resilience evaluation beyond averages. While some local outcomes were extreme, overall farm heterogeneity provided stability. Contrary to prior findings (Nelson et al., 2022) larger farm sizes did not consistently buffer variability, highlighting the dominant influence of weather and soil

variability and the more pervasive resilience challenge across farm sizes.

In this study, simulated yields showed lower interannual variability than observed data, a common outcome when models are calibrated to mean conditions rather than tuned for full variance representation. This likely reflects both the smoothing effects of synthetic weather generation and the omission of unmodelled stochastic events such as pest damage, machinery failure, or disease outbreaks, which contribute to observed yield variability. While the RLM and other PBMs that can be used within the framework have been previously calibrated and validated against long-term experimental data (e.g. Coleman et al., 2017), future work could refine calibrations to explicitly include variability metrics or benchmark results against multi-year field datasets for yield, N₂O emissions, and nitrate runoff. Such validation would strengthen the interpretation of modelled resilience indicators.

4.1. Methodological strengths and innovations

Our framework advances agroecosystem modelling by enabling farm-scale spatial (between-field) variation to be represented using simulated utilised areas (SUAs) as proxies for heterogeneous farm landscape units. By integrating spatial and temporal heterogeneity

Table 3

Description of exemplar sites. Each site represents a farm-scale management unit located within a 5 km water catchment, defined as including all waterbodies with $\geq 10\%$ of their area inside the 5 km buffer. Dominant robust farm types are from the UK Agricultural Survey. Soils are from NATMAP 1000 (covering $\geq 65\%$ of the catchment). Crops reflect dominant types (2018–2022) from the Land Cover+ Crops dataset.

Site Name	County, Region of England	Elevation / m	Catchment Area / km ²	Robust Farm Type	Dominant Soil Series (% of area ¹)	Dominant Crops (% arable land ²)
North Wyke (NW)	Devon, Southwest England	177	211.6 (4 water bodies)	Lowland Grazing Livestock	Hallsworth (19.9 %), Denbigh (8.5 %), Neath (8.5 %), Nercwys (8.0 %), Tedburn (7.5 %), Halstow (6.0 %), Crediton (5.1 %), Brickfield (3.7 %)	Grass Leys (29.7 %), Maize (13.2 %), Spring Barley (6.7 %), Winter Barley (11.9 %), Winter Wheat (22.4 %)
Rothamsted (RR)	Hertfordshire, East of England	128	340.5 (3 water bodies)	Cereals	Batcombe (26.2 %), Hornbeam (14.5 %), Carstens (6.7 %), Hamble (3.3 %), Windsor (3.2 %), Winchester (3.1 %), Hoo (2.9 %), Wickham (2.8 %), Charity (2.7 %)	Field Beans (6.7 %), Grass leys (7.2 %), OSR (8.4 %), Spring Barley (12.4 %), Spring Wheat (5.3 %), Winter Barley (10.2 %), Winter Wheat (33.5 %)

¹ Percentages shown until the cumulative total reaches $\geq 65\%$.

² Only crops covering $>5\%$ of arable land are listed.

through subsampling of soil types and crop sequences, we reintroduce stochasticity and therefore generate full outcome distributions, including emergent extremes. This supports more robust farm resilience assessments and helps identify rare risks masked by simpler deterministic approaches.

While the current implementation uses SUAs constructed from probabilistic combinations of field sizes, soils, and land uses, we recognise that in reality, field boundaries and soil types are spatially fixed, while management varies through time. Where detailed spatial datasets are available, the framework can readily incorporate actual field and soil boundaries, enabling management variation to be simulated directly on mapped units. The present approach, however, is motivated by the more common situation in which such detailed data are unavailable or incomplete. In this case, SUAs provide a derived analytical unit that allows consistent aggregation of field-scale model outputs to the farm scale and enables cross-site comparison under a unified structure.

The framework is flexible, modular, transparent, reproducible, and model-independent, enabling diverse agroecological questions and system comparisons. Whilst some advanced models such as DAESim (Taghikhah et al., 2022) and the unified process model developed by Sharma et al. (2025) integrate biophysical and data driven components, our approach focusses instead on harmonising spatially and temporally variable inputs and aggregating outputs to the decision-making scale. Our framework complements such models by providing a transferable cross-compatible structure for consistent comparison, model ensemble application, and systematic resilience assessment for research, policy, and practice.

Our approach lays a foundation for simulating multiple sources of farm-scale variation and assessing resilience more robustly. It accommodates model ensembles for exploring temporal variability and tipping points and for predicting a great range of outcomes (Hassall et al., 2022). While Pret et al. (2025) noted most modelling studies assess few resilience attributes, our framework can represent all five defined by Meuwissen et al. (2019): reserves (e.g. soil fertility, livestock), openness (input/output breadth), modularity (land use allocation), feedback tightness (mechanistically described in PBMs) and diversity (crop/livestock richness).

4.2. Limitations

Despite its strengths, several limitations remain. Process-based

models require detailed parameterisation of biophysical processes, and extensive data for calibration and evaluation. Our framework does not remove these demands but provides a transparent structure for documenting assumptions, harmonising inputs, and consistently representing sources of uncertainty across simulations.

Synthetic weather generators, while effective for typical climatic patterns, tend to underrepresent extremes (Semenov, 2008; Wilks and Wilby, 1999). This was evident in the reduced variance of generated vs observed weather at our exemplar sites, limiting assessments under extreme events and future climate scenarios. Integrating downscaled climate projections or hybrid weather generators could improve the representation of both typical and extreme conditions (Bhuvandas et al., 2014; Curceac et al., 2021).

The framework currently applies fixed crop sequences without dynamic or adaptive farmer decision-making. Real-world management often responds to in-season constraints or opportunities, like switching to spring wheat after failed autumn drilling—seen but not modelled at RR in 2021 (Fig. 9). Capturing such adaptive behaviour would require coupling the framework with rule- or agent-based decision models (El Fartassi et al., 2025). Real-world decisions also reflect financial factors. Incorporating economic models or multi-criteria optimisation would enhance the utility of our framework for actual decision support as opposed to more generic scenario exploration.

Our current implementation includes only field areas, omitting non-field components like yards, housing, and storage facilities, which can influence farm sustainability and resilience. While the framework captures spatial variation via field-level aggregation, it does not yet allow for interactions between fields (e.g., water and associated pollutant flow), nor post-harvest operations.

Finally, while management assumptions such as sowing dates, fertiliser application rates, and in-field practices were standardised here to reflect ‘typical’ conditions, these factors are often key determinants of yield variability. Future applications of the framework could incorporate sensitivity analyses or targeted scenario testing to quantify the influence of such management decisions and identify leverage points for improving best practices and resilience.

4.3. Future applications

The framework offers a robust foundation for capturing spatial and temporal heterogeneity in agroecosystems at scales relevant to farm management. Applying it to new regions, farming systems, and climate

performance and resilience metrics.

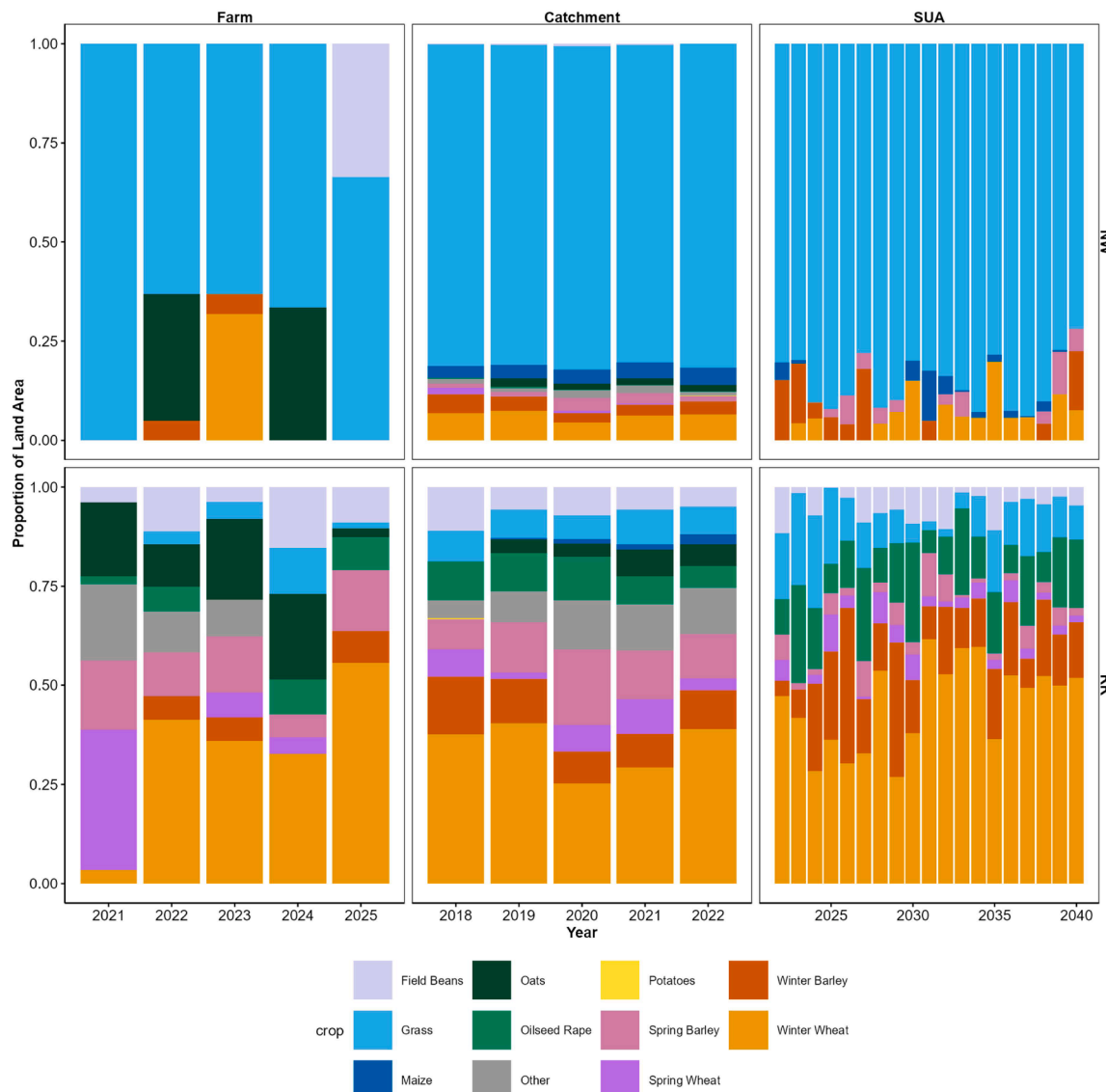


Fig. 9. Crop proportions for each site over time. Farm = records of cropped areas planted annually to each crop, which are harvested in the identified year. Catchment = total cropped areas within the WFD waterbodies identified by satellite data ([Land Cover plus: Crops, 2023](#)), SUA = An example medium-sized SUA, the total cropped area-time across all simulations (excluding fallow periods between crops).

scenarios could empower exploration of a wide range of resilience-focused questions, including multi-metric trade-offs, resilience mapping, and comparisons of adaptive strategies under varying environmental and policy contexts.

By explicitly representing multiple sources of input heterogeneity, the framework provides a generic method for harmonising model inputs and assimilating outputs at the farm scale. It can be integrated with diverse PBMs to test how incentivization through agricultural policy affects resilience or how farm structural and management diversity buffers climate extremes. Its ability to simulate outcome distributions under varied weather and management also supports applications in farm advisory services and risk planning.

Beyond the case studies presented here, the framework provides a transferable foundation for harmonised simulation and evaluation of resilience across diverse agroecosystem contexts and beyond. Because it is model-independent and based on structured, modular inputs, it can be readily adapted to other disciplines where spatial and temporal heterogeneity shape system performance at the decision-making scale, such

as forestry, aquaculture, or rangeland management. More broadly, it contributes to resilience science by operationalising a tractable, simulation-based approach to assess how input variability and system structure influence stability. By formalising how farm-scale variability can be represented, simulated, and analysed, it contributes to the ongoing development of reproducible modelling frameworks that link ecological, biophysical, and socio-environmental dimensions of resilience. In this way, our framework helps bridge process-based environmental models with resilience science, extending their combined value for research, policy, and decision support. The framework establishes a transferable, model-independent approach for exploring how within-farm heterogeneity shapes resilience, providing an essential methodological bridge between process-based modelling and real-world decision-making.

CRediT authorship contribution statement

Helen Metcalfe: Writing – review & editing, Writing – original draft,

Visualization, Validation, Software, Methodology, Investigation, Funding acquisition, Formal analysis, Conceptualization. **Kevin Coleman:** Writing – review & editing, Writing – original draft, Visualization, Validation, Software, Methodology, Investigation, Formal analysis, Conceptualization. **Yusheng Zhang:** Writing – review & editing, Writing – original draft, Validation, Methodology, Investigation, Conceptualization. **Prakash N Dixit:** Writing – review & editing, Methodology, Investigation, Conceptualization. **Sana Saeed:** Writing – review & editing, Visualization, Methodology, Formal analysis, Data curation. **Andrew Mead:** Writing – review & editing, Writing – original draft, Visualization, Validation, Supervision, Methodology, Formal analysis, Data curation. **Adrian L Collins:** Writing – review & editing, Supervision, Resources, Project administration, Methodology, Investigation, Funding acquisition, Conceptualization.

Declaration of competing interest

The authors declare the following financial interests/personal relationships which may be considered as potential competing interests: Adrian L Collins reports financial support was provided by Biotechnology and Biological Sciences Research Council. If there are other authors, they declare that they have no known competing financial interests or personal relationships that could have appeared to influence the work reported in this paper.

Acknowledgements

The authors would like to thank Nimai Senapati and Mikhail Semenov for their support with the analysis of LARS-WG generated weather data. Rothamsted Research receives strategic funding from the UKRI (UK Research and Innovation) Biotechnology and Biological Sciences Research Council (UKRI-BBSRC). We gratefully acknowledge support from the Resilient Farming Futures Institute Strategic Programme [BB/X010961/1; BBS/E/RH/230004A].

Supplementary materials

Supplementary material associated with this article can be found, in the online version, at [doi:10.1016/j.ecolmodel.2025.111432](https://doi.org/10.1016/j.ecolmodel.2025.111432).

Data availability

No data was used for the research described in the article.

References

Abrahamsen, P., Hansen, S., 2000. Daisy: an open soil-crop-atmosphere system model. *Environ. Model. Softw.* 15 (3), 313–330. [https://doi.org/10.1016/s1364-8152\(00\)0003-7](https://doi.org/10.1016/s1364-8152(00)0003-7).

AfricaFertilizer, 2015. AfricaFertilizer Database [Online] Retrieved 23/06/2025 from. <https://africafertilizer.org/#/en>.

Allen, R.G., Pereira, L.S., Raes, D., Smith, M., 1998. *Crop Evapotranspiration - Guidelines for Computing Crop Water Requirements - FAO Irrigation and Drainage Paper 56*.

Avery, B.W., 1980. Soil classification for England and Wales (Higher categories). Soil Survey, Technical Monograph No. 14. Rothamsted Experimental Station, Harpenden, England.

Avery, B.W., Catt, J.A., 1995. The Soil at Rothamsted. *Lawes Agricultural Trust*.

Avery, B.W., Catt, J.A., Coleman, K., Pino-Chandia, L., & Ostler, R. (2024). *Soil Map of Rothamsted Estate* (<https://doi.org/10.23637/rothamsted.98z89>).

Barrett, T., Dowie, M., Srinivasan, A., Gorecki, J., Chirico, M., Hocking, T., Schwendinger, B., Krylov, I., 2025. data.table: Extension of 'data.frame'. R Package Version 1.17.99. <https://r-databatable.com>.

Beillouin, D., Ben-Ari, T., Makowski, D., 2019. Evidence map of crop diversification strategies at the global scale. *Environ. Res. Lett.* 14 (12), 123001. <https://doi.org/10.1088/1748-9326/ab4449>.

Bengtsson, H., 2021. A Unifying Framework for Parallel and Distributed Processing in R using Futures. *R. J.* 13 (2), 208–227. <https://doi.org/10.32614/RJ-2021-048>.

Bhuvandas, N., Timbadiya, P.V., Patel, P.J., Porey, P.D., 2014. Review of downscaling methods in climate change and their role in hydrological studies. *Int. J. Environ. Ecol. Geol. Mar. Eng.* 8, 713–718.

Biggs, R., Gordon, L., Raudsepp-Hearne, C., Schlüter, M., Walker, B., 2015. Principle 3 – manage slow variables and feedbacks. In: Biggs, R., Schlüter, M., Schoon, M.L. (Eds.), *Principles For Building Resilience: Sustaining Ecosystem Services in Social-Ecological Systems*. Cambridge University Press, pp. 105–141. <https://doi.org/10.1017/CBO9781316014240.006>.

Calzadilla, A., Rehdanz, K., Betts, R., Falloon, P., Wiltshire, A., Tol, R.S.J., 2013. Climate change impacts on global agriculture. *Clim. Change* 120 (1), 357–374. <https://doi.org/10.1007/s10584-013-0822-4>.

Coleman, K., Jenkinson, D.S., 2014. *RothC - A Model For the Turnover of Carbon in Soil: Model Description and Users Guide (updated June 2014)*. Lawes Agricultural Trust.

Coleman, K., Muhammed, S.E., Milne, A.E., Todman, L.C., Dailey, A.G., Glendining, M.J., Whitmore, A.P., 2017. The landscape model: a model for exploring trade-offs between agricultural production and the environment. *Sci. Total Environ.* 609, 1483–1499. <https://doi.org/10.1016/j.scitotenv.2017.07.193>.

Conway, G.R., 1987. The properties of agroecosystems. *Agric. Syst.* 24 (2), 95–117.

CSIRO, 2024. Australian Soil Resource Information System Website. v1. CSIRO, Data Collection. <https://doi.org/10.25919/pdct-9a97>. Retrieved 10 July 2025 from.

Curcecu, S., Milne, A., Atkinson, P.M., Wu, L., Harris, P., 2021. Elucidating the performance of hybrid models for predicting extreme water flow events through variography and wavelet analyses. *J. Hydrol.* 598, 126442. <https://doi.org/10.1016/j.jhydrol.2021.126442>.

Darnhofer, I., John, F., Moller, H., 2010. Assessing a farm's sustainability: insights from resilience thinking. *Int. J. Agric. Sustain.* 8 (3), 186–198. <https://doi.org/10.3763/ijas.2010.0480>.

Davoudi, S., Keith, S., Jamila, H.L., E, Q.A., D, P.G., Cathy, W., Hartmut, F., Darryn, M., Libby, P., Davoudi, S., 2012. Resilience: a bridging concept or a dead end? “Reframing” resilience: challenges for planning theory and practice interacting traps: resilience assessment of a pasture management system in Northern Afghanistan urban resilience: what does it mean in planning practice? Resilience as a useful concept for climate change adaptation? The politics of resilience for planning: a cautionary note. *Plan. Theory. Pract.* 13 (2), 299–333. <https://doi.org/10.1080/14649357.2012.677124>.

Defra, 2019. *British Survey of Fertiliser Practice2018 - Fertiliser use On Farm Crops For Crop Year 2018*.

Defra, 2020. *British Survey of Fertiliser Practice 2019 - Fertiliser use On Farm Crops For Crop Year 2019*.

Defra, 2021a. *British Survey of Fertiliser Practice2020 - Fertiliser use On Farm Crops For Crop Year 2020*.

Defra, 2021b. Structure of the Agricultural Industry in England and the UK At June. Retrieved 25 June 2025 from. <https://www.gov.uk/government/statistical-data-sets/structure-of-the-agricultural-industry-in-england-and-the-uk-at-june>.

Defra, 2022. *British Survey of Fertiliser Practice 2021 - Fertiliser use On Farm Crops For Crop Year 2021*.

Defra, 2023. *British Survey of Fertiliser Practice 2022 - Fertiliser use On Farm Crops For Crop Year 2022*.

Defra, 2025a. Catchment Data Explorer. Retrieved 3 July 2025 from. <https://environment.data.gov.uk/catchment-planning>.

Defra, 2025b. Farm Business Survey. Retrieved 3 July 2025 from. <https://www.farmbusinesssurvey.co.uk/>.

Defra, 2025c. Farm Practices Survey February 2025. Retrieved 10 July 2025 from. <https://www.gov.uk/government/statistics/farm-practices-survey-february-2025>.

Döring, T.F., Reckling, M., 2018. Detecting global trends of cereal yield stability by adjusting the coefficient of variation. *Eur. J. Agron.* 99, 30–36. <https://doi.org/10.1016/j.eja.2018.06.007>.

El Fartassi, I., Milne, A.E., Metcalfe, H., El Alami, R., Diarra, A., Alonso-Chavez, V., Zawadzka, J., Waine, T.W., Corstanje, R., 2025. An agent-based model of farmer decision making: application to shared water resources in Arid and semi-arid regions. *Agric. Water. Manage.* 310, 109357. <https://doi.org/10.1016/j.agwat.2025.109357>.

Elmqvist, T., Folke, C., Nyström, M., Peterson, G., Bengtsson, J., Walker, B., Norberg, J., 2003. Response diversity, ecosystem change, and resilience. *Front. Ecol. Environ.* 1 (9), 488–494. [https://doi.org/10.1890/1540-9295\(2003\)001\[0488:RDECAR\]2.0.CO;2](https://doi.org/10.1890/1540-9295(2003)001[0488:RDECAR]2.0.CO;2).

European Commission, 2025. The JRC MARS Agro-Meteorological Database Provides Gridded Daily Agro-Meteorological Data At 25 Km Grid Resolution from 1979 to the Last Calendar Year completed, For the European Union and Neighbouring Countries. Joint Research Centre European Commission. Retrieved 23/06/2025 from. <https://agri4cast.jrc.ec.europa.eu/dataportal>.

FAO, 2020. FAOSTAT [Online]. Retrieved 10 July 2025 from. <https://www.fao.org/faostat/en/#home>.

Folke, C., Carpenter, S.R., Walker, B., Scheffer, M., Chapin, T., Rockström, J., 2010. Resilience thinking: integrating resilience, adaptability and transformability. *Ecol. Soc.* 15 (4), 20.

Gilttrap, D., Li, C., Sagar, S., 2010. DNDC: a process-based model of greenhouse gas fluxes from agricultural soils. *Agric. Ecosyst. Environ.* 136 (3–4), 292–300. <https://doi.org/10.1016/j.agee.2009.06.014>.

Government of India, 2025. Agricultural Census. Retrieved 02 July 2025 from. <https://www.data.gov.in/sector/Agriculture>.

Grimm, V., Augusiak, J., Focks, A., Frank, B., Gabsi, F., Johnston, A., Liu, C., Martin, B., Meli, M., Radchuk, V., Thorbek, P., Railsback, S., 2014. Towards better modelling and decision support: documenting model development, testing, and analysis using TRACE. *Ecol. Model.* 280, 129–139. <https://doi.org/10.1016/j.ecolmodel.2014.01.018>.

Hassall, K.L., Coleman, K., Dixit, P.N., Granger, S.J., Zhang, Y., Sharp, R.T., Wu, L., Whitmore, A.P., Richter, G.M., Collins, A.L., Milne, A.E., 2022. Exploring the effects of land management change on productivity, carbon and nutrient balance: application of an Ensemble Modelling Approach to the upper River Taw observatory,

UK. Sci. Total Environ. 824, 153824. <https://doi.org/10.1016/j.scitotenv.2022.153824>.

Hengl, T., Mendes de Jesus, J., Heuvelink, G.B.M., Ruiperez Gonzalez, M., Kilibarda, M., Blagotić, A., Shangguan, W., Wright, M.N., Geng, X., Bauer-Marschallinger, B., Guevara, M.A., Vargas, R., MacMillan, R.A., Batjes, N.H., Leenaars, J.G.B., Ribeiro, E., Wheeler, I., Mantel, S., Kempen, B., 2017. SoilGrids250m: global gridded soil information based on machine learning. *PLoS One* 12 (2), e0169748. <https://doi.org/10.1371/journal.pone.0169748>.

Holling, C.S., 1973. Resilience and Stability of Ecological Systems. *Annu Rev. Ecol. Evol. Syst.* 4 (1973), 1–23. <https://doi.org/10.1146/annurev.es.04.110173.000245>.

Holzworth, D., Huth, N., Devoil, P., Zurcher, E., Herrmann, N., McLean, G., Chen, K., van Oosterom, E., Snow, V., Murphy, C., Moore, A., Brown, H., Whish, J., Verrall, S., Fainges, J., Bell, L., Peake, A., Poulton, P., Hochman, Z., Keating, B., 2014. APSIM - Evolution towards a new generation of agricultural systems simulation. *Environ. Model. Softw.* 62, 327–350. <https://doi.org/10.1016/j.envsoft.2014.07.009>.

Hoy, C.W., 2015. Agroecosystem health, agroecosystem resilience, and food security. *J. Environ. Stud. Sci.* 5 (4), 623–635. <https://doi.org/10.1007/s13412-015-0322-0>.

IBGE, 2017. *Censo Agropecuário. Instituto Brasileiro De Geografia e Estatística*.

Jakeman, A., Letcher, R., Norton, J., 2006. Ten iterative steps in development and evaluation of environmental models. *Environ. Model. Softw.* 21 (5), 602–614. <https://doi.org/10.1016/j.envsoft.2006.01.004>.

Jakeman, A.J., Elsawah, S., Wang, H.-H., Hamilton, S.H., Melsen, L., Grimm, V., 2024. Towards normalizing good practice across the whole modeling cycle: its instrumentation and future research topics. *Socio-Environ. Syst. Modell.* 6, 18755. <https://doi.org/10.18174/sesmo.18755>.

Jentsch, M.F., James, P.A.B., Bourikas, L., Bahaj, A.S., 2013. Transforming existing weather data for worldwide locations to enable energy and building performance simulation under future climates. *Renew. Energy* 55, 514–524. <https://doi.org/10.1016/j.renene.2012.12.049>.

Jones, P.G., Thornton, P.K., 2013. Generating downscaled weather data from a suite of climate models for agricultural modelling applications. *Agric. Syst.* 114, 1–5. <https://doi.org/10.1016/j.agry.2012.08.002>.

Kleinman, P.J.A., Spiegel, S., Rigby, J.R., Goslee, S.C., Baker, J.M., Bestelmeyer, B.T., Boughton, R.K., Bryant, R.B., Cavigelli, M.A., Derner, J.D., Duncan, E.W., Goodrich, D.C., Huggins, D.R., King, K.W., Liebig, M.A., Locke, M.A., Mirsky, S.B., Moglen, G.E., Moorman, T.B., Walther, C.L., 2018. Advancing the Sustainability of US Agriculture through Long-Term Research. *J. Environ. Qual.* 47 (6), 1412–1425. <https://doi.org/10.2134/jeq2018.05.0171>.

Kotschy, K., Biggs, R., Daw, T., Folke, C., West, P.C., 2015. Principle 1 – maintain diversity and redundancy. In: Biggs, R., Schlüter, M., Schoon, M.L. (Eds.), *Principles For Building Resilience: Sustaining Ecosystem Services in Social-Ecological Systems*. Cambridge University Press, pp. 50–79. <https://doi.org/10.1017/CBO9781316014240.004>.

Laal, R., 2021. Chapter 31 - Climate change and agriculture. In: Letcher, T.M. (Ed.), *Climate Change*, 3rd ed. Elsevier, pp. 661–686. <https://doi.org/10.1016/B978-0-12-821575-3.00031-1>.

Land Cover plus: Crops, 2023. [FileGeoDatabase Geospatial data], Scale 1:2500, Tiles: GB, Updated: 29 January 2024, CEH, Using: EDINA Environment Digimap Service. < <https://digimap.edina.ac.uk> > Downloaded: 2024-05-20 12:43:54.166.

LandIS, 2024. National Soil Map of England and Wales - NATMAP. Retrieved 25 June 2025 from. <https://www.landis.org.uk/data/nm1000.cfm>.

Lin, B.B., 2011. Resilience in agriculture through crop diversification: adaptive management for environmental change. *Bioscience* 61 (3), 183–193. <https://doi.org/10.1525/bio.2011.61.3.4>.

Marston, C., Rowland, C.S., Neil, A.W., Morton, R.D., 2022. *Land Cover Map 2021 (Land Parcels, GB)*. (NERC EDS Environmental Information Data Centre).

Melchior, I.C., Newig, J., 2021. Governing transitions towards sustainable agriculture—taking stock of an emerging field of research. *Sustainability* 13 (2), 528.

Menne, M.J., Durre, I., Vose, R.S., Gleason, B.E., Houston, T.G., 2012. An overview of the global historical climatology network-daily database. *J. Atmos. Ocean. Technol.* 29 (7), 897–910. <https://doi.org/10.1175/JTECH-D-11-0013.1>.

Met office, 2025. Historic Station Data. Met office. Retrieved 9 July 2025 from. <https://www.metoffice.gov.uk/research/climate/maps-and-data/historic-station-data>.

Meuwissen, M., Feindt, P., Spiegel, A., Termeer, C., Mathijs, E., de Mey, Y., Finger, R., Balmann, A., Wauters, E., Urquhart, J., Vigani, M., Zawalinska, K., Herrera, H., Nicholas-Davies, P., Hansson, H., Paas, W., Slipper, T., Coopmans, I., Vroege, W., Reidsma, P., 2019. A framework to assess the resilience of farming systems. *Agric. Syst.* 176, 102656. <https://doi.org/10.1016/j.agry.2019.102656>.

Nelson, K.S., Patalee, B., Yao, B., 2022. Higher landscape diversity associated with improved crop production resilience in Kansas-USA. *Environ. Res. Lett.* 17 (8), 084011. <https://doi.org/10.1088/1748-9326/ac7e5f>.

Olivoto, T., Lúcio, A.D.C., 2020. metan: an R package for multi-environment trial analysis. *Methods Ecol. Evol.* 11 (6), 783–789. <https://doi.org/10.1111/2041-210X.13384>.

Orehova, T., Ischuk, Y., 2023. The risks and challenges of agricultural products global market. *Herald of Khmelnytskyi National University Econ. Sci.* 320 (4), 119–124. <https://doi.org/10.31891/2307-5740-2023-320-4-17>.

Orr, R.J., Murray, P.J., Eyles, C.J., Blackwell, M.S.A., Cardenas, L.M., Collins, A.L., Dungait, J.A.J., Goulding, K.W.T., Griffith, B.A., Gurr, S.J., Harris, P., Hawkins, J.M.B., Misselbrook, T.H., Rawlings, C., Shepherd, A., Sint, H., Takahashi, T., Tozer, K.N., Whitmore, A.P., Lee, M.R.F., 2016. The North Wyke Farm Platform: effect of temperate grassland farming systems on soil moisture contents, runoff and associated water quality dynamics. *Eur. J. Soil. Sci.* 67 (4), 374–385. <https://doi.org/10.1111/ejss.12350>.

Parton, W.J., Schimek, D.S., Ojima, D.S., Cole, C.V., 1994. A general model for soil organic matter dynamics: sensitivity to litter chemistry, texture and management. In:

Bryant, R.B., Arnold, R.W. (Eds.), *Quantitative Modeling of Soil Forming Processes. SSSA Special Publication 39*, pp. 147–167.

Pret, V., Falconnier, G.N., Affholder, F., Corbeels, M., Chikowo, R., Descheemaeker, K., 2025. Farm resilience to climatic risk: A review. *Agron. Sustain. Dev.* 45 (1), 10. <https://doi.org/10.1007/s13593-024-00998-w>.

R Core Team, 2025. R: A language and Environment For Statistical Computing (Version 4.4.1) [Computer Software]. <https://www.R-project.org/>.

Rao, N.H., Katyal, J.C., Reddy, M.N., 2004. Embedding the sustainability perspective into agricultural research: implications for research management. *Outlook Agric.* 33 (3), 167–176. <https://doi.org/10.5367/0000000042530141>.

Ren, W., 2019. Towards an integrated agroecosystem modeling approach for climate-smart agriculture management. Bridging Among Disciplines By Synthesizing Soil and Plant Processes, pp. 127–144. <https://doi.org/10.2134/advagricsystmodel8.2018.0004>.

Scheffer, M., Bascompte, J., Brock, W.A., Brovkin, V., Carpenter, S.R., Dakos, V., Held, H., van Nes, E.H., Rietkerk, M., Sugihara, G., 2009. Early-warning signals for critical transitions. *Nature* 461 (7260), 53–59. <https://doi.org/10.1038/nature08227>.

Scott, M., 2013. Resilience: a Conceptual Lens for Rural Studies? *Geogr. Compass.* 7 (9), 597–610. <https://doi.org/10.1111/gec3.12066>.

Semenov, M.A., 2008. Simulation of extreme weather events by a stochastic weather generator. *Clim. Res.* 35, 203–212.

Semenov, M.A., Barrow, E.M., 1997. Use of a stochastic weather generator in the development of climate change scenarios. *Clim. Change* 35 (4), 397–414.

Semenov, M.A., Barrow, E.M., 2002. LARS-WG: A Stochastic Weather Generator For Use in Climate Impact Studies (Version 3.0 User Manual).

Semenov, M.A., Senapati, N., Coleman, K., Collins, A.L., 2024. A dataset of CMIP6-based climate scenarios for climate change impact assessment in Great Britain. *Data Br.* 55, 110709. <https://doi.org/10.1016/j.dib.2024.110709>.

Sharma, P., Gyalog, G., Varga, M., 2025. Unified process model-based assessment of environmental interactions and ecosystem services of a managed fishpond-reed agroecosystem. *Ecol. Model.* 506, 111151. <https://doi.org/10.1016/j.ecolmodel.2025.111151>.

Sharp, R.T., Henrys, P.A., Jarvis, S.G., Whitmore, A.P., Milne, A.E., Coleman, K., Mohankumar, S.E.P., Metcalfe, H., 2021. Simulating cropping sequences using earth observation data. *Comput. Electron. Agric.* 188, 106330. <https://doi.org/10.1016/j.compag.2021.106330>.

Sharp, R.T., Sanderson Bellamy, A., Clear, A., Mitchell Finnigan, S., Furness, E., Meador, E., Metcalfe, H., Mills, S., Coleman, K., Whitmore, A.P., Milne, A.E., 2024. Implications and impacts of aligning regional agriculture with a healthy diet. *J. Clean. Prod.* 249, 141375. <https://doi.org/10.1016/j.jclepro.2024.141375>.

Taghikhah, F., Borevitz, J., Costanza, R., Voinov, A., 2022. DAESim: a dynamic agro-ecosystem simulation model for natural capital assessment. *Ecol. Model.* 468, 109930. <https://doi.org/10.1016/j.ecolmodel.2022.109930>.

Thiombiano, L., Yemefack, M., Van Ranst, E., Spaargaren, O., Michel, E., Kilasara, M., Montanarella, L., Jones, R., Hallett, S., Dampha, A., Gallali, T., Deckers, J., Breuning-Madsen, H., Jones, A., Brossard, M., Jones, A., Le Roux, P., Dewitte, O., Jones, R., Zougnoré, R., 2013. Soil Atlas of Africa. Publications Office. <https://doi.org/10.2788/52319>.

Thornton, M.M., Shrestha, R., Wei, Y., Thornton, P.E., Kao, S.C., 2022. Daymet: Station-Level Inputs and Cross-Validation for North America, Version 4 R1. ORNL Distributed Active Archive Center.

USDA, 2022. Census of Agriculture. Retrieved 19 June 2025 from. https://www.nass.usda.gov/Publications/AgCensus/2022/index.php#full_report.

USDA, 2025. Web Soil Survey. Retrieved 23/06/2025 from. <https://websoilsurvey.scegov.usda.gov/App/HomePage.htm>.

Van Engelen, V., Verdoordt, A., Dijkshoorn, K., Van Ranst, E., 2006. Soil and Terrain Database of Central Africa-DR of Congo, Burundi and Rwanda Report, 2006/07. <http://www.issrc.org>.

International, V.S.N., 2023. Genstat For Windows, 23rd Edition. (Version 23rd) Genstat.co.uk.

Walker, B., Hollin, C.S., Carpenter, S.R., Kinzig, A., 2004. Resilience, adaptability and transformability in social-ecological systems. *Ecol. Soc.* 9 (2), 5.

Wang, H.-H., van Voorn, G., Grant, W.E., Zare, F., Giupponi, C., Steinmann, P., Müller, B., Elsawah, S., van Delden, H., Athanasiadis, I.N., Sun, Z., Jager, W., Little, J.C., Jakeman, A.J., 2023. Scale decisions and good practices in socio-environmental systems modelling: guidance and documentation during problem scoping and model formulation. *Socio-Environ. Syst. Modell.* 5, 18563. <https://doi.org/10.18174/sesmo.18563>.

Wickham, H., 2016. *Elegant Graphics For Data Analysis*, 2nd ed.

Wickham, H., François, R., Henry, L., Müller, K., Vaughan, D., 2025. dplyr: A Grammar of Data Manipulation. R Package Version 1.1.4. <https://dplyr.tidyverse.org>.

Wilks, D.S., Wilby, R.L., 1999. The weather generation game: a review of stochastic weather models. *Progr. Phys. Geogr.* 23 (3), 329–357. <https://doi.org/10.1177/030913339902300302>.

Wolf, J., 2012. *User Guide For LINTUL4 and LINTUL4V: Simple generic Model For Simulation of Crop Growth Under potential, Water Limited and Nitrogen Limited Conditions*.

Wösten, J.H.M., Lilly, A., Nemes, A., Le Bas, C., 1999. Development and use of a database of hydraulic properties of European soils. *Geoderma* 90 (3–4), 169–185. [https://doi.org/10.1016/s0016-7061\(98\)00132-3](https://doi.org/10.1016/s0016-7061(98)00132-3).

Xie, H., Li, J., Li, T., Lu, X., Hu, Q., Qin, Z., 2025. GloRice, a global rice database (v1.0): I. Gridded paddy rice annual distribution from 1961 to 2021. *Sci. Data* 12 (1), 182. <https://doi.org/10.1038/s41597-025-04483-1>.

Yang, Y., Tilman, D., Jin, Z., Smith, P., Barrett, C.B., Zhu, Y.-G., Burney, J., D'Odorico, P., Fantke, P., Fargione, J., Finlay, J.C., Rulli, M.C., Sloat, L., Jan van Groenigen, K.,

West, P.C., Ziska, L., Michalak, A.M., Team, t.C.-A., Lobell, D.B., Zhuang, M., 2024. Climate change exacerbates the environmental impacts of agriculture. *Science* 385 (6713), eadn3747. <https://doi.org/10.1126/science.adn3747>.

Yatagai, A., Kamiguchi, K., Arakawa, O., Hamada, A., Yasutomi, N., Kitoh, A., 2012. APHRODITE: constructing a Long-Term Daily Gridded Precipitation Dataset for Asia

Based on a Dense Network of Rain Gauges. *Bull. Am. Meteorol. Soc.* 93 (9), 1401–1415. <https://doi.org/10.1175/BAMS-D-11-00122.1>.

Zhang, Y., Wu, L., Jebari, A., Collins, A., 2024. Impacts of reduced synthetic fertiliser use under current and future climates: exploration using integrated agroecosystem modelling in the upper River Taw observatory, UK. *J. Environ. Manage.* 351, 119732. <https://doi.org/10.1016/j.jenvman.2023.119732>.